HAL open science

Paleoproterozoic crustal evolution and Mesoproterozoic overprint in the Roosevelt-Guariba Transpressive Belt, Juruena Terrain, Southeastern Amazonas, Brazil

Marcelo E Almeida, Antonio Charles Oliveira, Joao Orestes Santos, Joseneusa B Rodrigues, Gilles Ruffet

▶ **To cite this version:**

Marcelo E Almeida, Antonio Charles Oliveira, Joao Orestes Santos, Joseneusa B Rodrigues, Gilles Ruffet. Paleoproterozoic crustal evolution and Mesoproterozoic overprint in the Roosevelt-Guariba Transpressive Belt, Juruena Terrain, Southeastern Amazonas, Brazil. Journal of the Geological Survey of Brazil, 2022, 5 (3), pp.221 - 249. 10.29396/jgsb.2022.v5.n3.5 . insu-03968167

HAL Id: insu-03968167

https://insu.hal.science/insu-03968167

Submitted on 1 Feb 2023

HAL is a multi-disciplinary open access archive for the deposit and dissemination of scientific research documents, whether they are published or not. The documents may come from teaching and research institutions in France or abroad, or from public or private research centers.

L'archive ouverte pluridisciplinaire **HAL**, est destinée au dépôt et à la diffusion de documents scientifiques de niveau recherche, publiés ou non, émanant des établissements d'enseignement et de recherche français ou étrangers, des laboratoires publics ou privés.

Distributed under a Creative Commons Attribution 4.0 International License

Journal of the Geological Survey of Brazil

Paleoproterozoic crustal evolution and Mesoproterozoic overprint in the Roosevelt-Guariba Transpressive Belt, Juruena Terrain, Southeastern Amazonas, Brazil

Marcelo E. Almeida[1*], Antonio Charles da S. Oliveira[2,3], João Orestes S. Santos[4], Joseneusa B. Rodrigues[5], Gilles Ruffet[6]

[1]Geological Survey of Brazil-CPRM, Av. Pasteur 404, Urca, Rio de Janeiro, RJ, Brazil, CEP 22290-255
[2]Geological Survey of Brazil-CPRM, Av. André Araújo 2160, Aleixo, Manaus, AM, Brazil, CEP 69060-001,
[3]Department of Geosciences, Postgraduate Program, Federal University of Amazonas, Av. General Rodrigo Otávio, nº 6.200, Campus Universitário Senador Arthur Virgílio Filho, Setor Norte, Coroado I, CEP: 69077-000, Manaus, Amazonas, Brazil
[4]University of Western Australia, 35 Stirling Highway Perth WA 6009, Australia
[5]Geological Survey of Brazil-CPRM, Setor Bancário Norte - SBN Quadra 02, Bloco H - Asa Norte, Ed. Central Brasília, Brasília, DF, Brazil, CEP 70040-904
[6]CNRS (CNRS/INSU) UMR 6118, Université de Rennes I, Géosciences Rennes, 35042 Rennes Cedex, France

Abstract

The Juruena Terrain (Rondônia-Juruena Province) in the southeastern Amazonas State shows a NW-SE dextral shear zones system denominated Roosevelt-Guariba Transpressive Belt (RGTB). The RGTB was generated in response to intracontinental crustal reworking, juxtaposing Paleoproterozoic Juruena granitic-gneiss and coeval supracrustal associations. This granitic-gneiss basement shows high-K calc-alkaline (Teodósia Suite) to transitional I- to A-type (Igarapé das Lontras Suite) signatures, produced in a continental magmatic arc setting around 1760-1740 Ma (zircon, titanite; U-Pb SHRIMP, LA-ICP-MS). New geochronological data about of the deformation and metamorphic rocks in the RGTB were obtained from migmatite paragneisses, amphibolites, S-type leucogranite (Quatro Cachoeiras Complex and Itamaraty Suite; zircon U-Pb SHRIMP) and protomylonites and mylonites (Igarapé das Lontras and Teodosia protoliths; amphibole-muscovite-sericite Ar-Ar step heating). The results suggest that Southeastern Amazonas (northern Juruena Terrain) was metamorphosed/deformed during 1530-1460 Ma under temperatures of 900°C (zircon) to 580°C (hornblende) and 420°C (muscovite). The geochronological data show that the granite-gneiss basement (continental magmatic arc) and supracrustal rocks (foreland basin) were reworked by a regional event with an age interval of 1530 Ma (high grade and anatexis) to 1460 Ma (medium grade). Finally, the Juruena Terrain is affected by a younger low-T event (1300 Ma, muscovite Ar-Ar step heating) with wide NE-trending structures (e.g. Buiuçu Shear Zone). This 1.3 Ga event suggests a continental reactivation caused by the pericratonic deformation related to Candeias/Sunsás Orogeny during the Columbia Supercontinent break-up, before the Rodinia Supercontinent assembly. In summary, the Juruena Terrain in the southeast Amazonas shows a complex metamorphic and structural intracontinental evolution, involving polycyclic events from late Orosirian to Ectasian in a convergent tectonic setting. Therefore, the Juruena Terrain shows similar accretionary histories with other orogens and has apparent long-lived connections with Laurentia (Yavapai Province) and Baltica (Transscandinavian Igneous Belt), forming the core of the Columbia Supercontinent.

Article Information

Publication type: Research Papers
Received 3 June 2022
Accepted 9 November 2022
Online pub. 11 November 2022
Editor: Henri Masquelin

Keywords:
Rondônia-Juruena,
Southeastern Amazonas,
Tectonothermal Events,
Geochronology

*Corresponding author
Marcelo E Almeida
marcelo.esteves@sgb.gov.br

1. Introduction

The Precambrian basement exposed in the southeast Amazonas State, Brazil (southern Amazon Craton, Figure 1) is represented mainly by granitic-gneiss and locally by supracrustal associations (e.g. Almeida et al. 2016; Oliveira and Lira 2019), originally included in the Rio Negro-Juruena (1.80-1.55 Ga, Tassinari et al. 1996) or later in Rondônia-Juruena Province (1.80-1.53 Ga, Santos et al. 2000). The orthoderived basement is interpreted as an accretionary crustal domain (Tassinari et al. 2000) generated in the final stages of a 1.85-1.73 Ga magmatic arc system (Juruena Accretionary Belt; Scandolara et al. 2016). This granite-gneiss basement is composed of the Teodósia (high-K calc-alkaline, HFSE-enriched) and Igarapé das Lontras (transitional I-type to aluminous A-type) suites (Figure 2). The supracrustal

This work is licensed under a Creative Commons Attribution 4.0 Internacional License.

ISSN: 2595-1939
https://doi.org/10.29396/jgsb.2022.v5.n3.5
Open access at jgsb.cprm.gov.br

rocks (Quatro Cachoreiras Complex) are related to the pre- to syncollisional stages of this accretionary belt (Oliveira 2016).

In the same region, Calymmian intrusions of subalkaline A-type and rapakivi granites (Serra da Providência Suite; 1.54-1.51 Ga) are associated with quartz monzonites and gabbronorites, including coeval (sub)volcanic rocks of the Serra do Gavião Group (Oliveira and Lira 2019; Oliveira 2016; Figure 2). Also in Mesoproterozoic times (Ectasian) there is evidence of the reworking of the Rondônia-Juruena Province by a thermotectonic event related to the Rondonian-San Inácio/ Cachoeirinha Orogeny (1.50-1.30 Ga). This collisional event at 1.37-1.35 Ga (Teixeira et al. 1989; Bettencourt et al, 1999; Santos et al. 2003; Scandolara et al. 2011) shows also felsic intrusions, in this case, related to the orogenic collapse and extensional phase (Alto Candeias, 1.34 Ga; São Lourenço-Caripunas, 1.31 Ga). In the southeast Amazonas State, this collisional event was not recognized until now and the tectonothermal effects are not so well understood. However, structural geophysical analysis and multiscale study suggest a crustal evolution model based on Paleoproterozoic accretion and intracontinental Mesoproterozoic tectonothermal events affecting the Juruena Terrain in this region (Oliveira and Almeida 2021). "Terrain' is used here as a descriptive term to refer to an area having a preponderance of a particular rock or group of rocks.

The study area in the southeast Amazonas State (Figure 2) encompasses the northern part of the Juruena Terrain (Scandolara et al. 1999), mainly in the Aripuanã, Roosevelt and Guariba River basins. In this paper, we present new U-Pb SHRIMP geochronological data (zircon and titanite) of calc-alkaline basement (Teodósia Suite, Juruena Complex), supracrustal rocks (Quatro Cachoeiras Complex), two-mica granite (Itamarati Suite), and new Ar-Ar step heating ages (muscovite and hornblende) of granites and sheared subvolcanic rocks (Colíder Group, Teodósia Suite and Igarapé das Lontras Suite). The aim is to show how Mesoproterozoic events affected the Paleoproterozoic basement of this region, seeking to shed light on the discussion about the magmatic

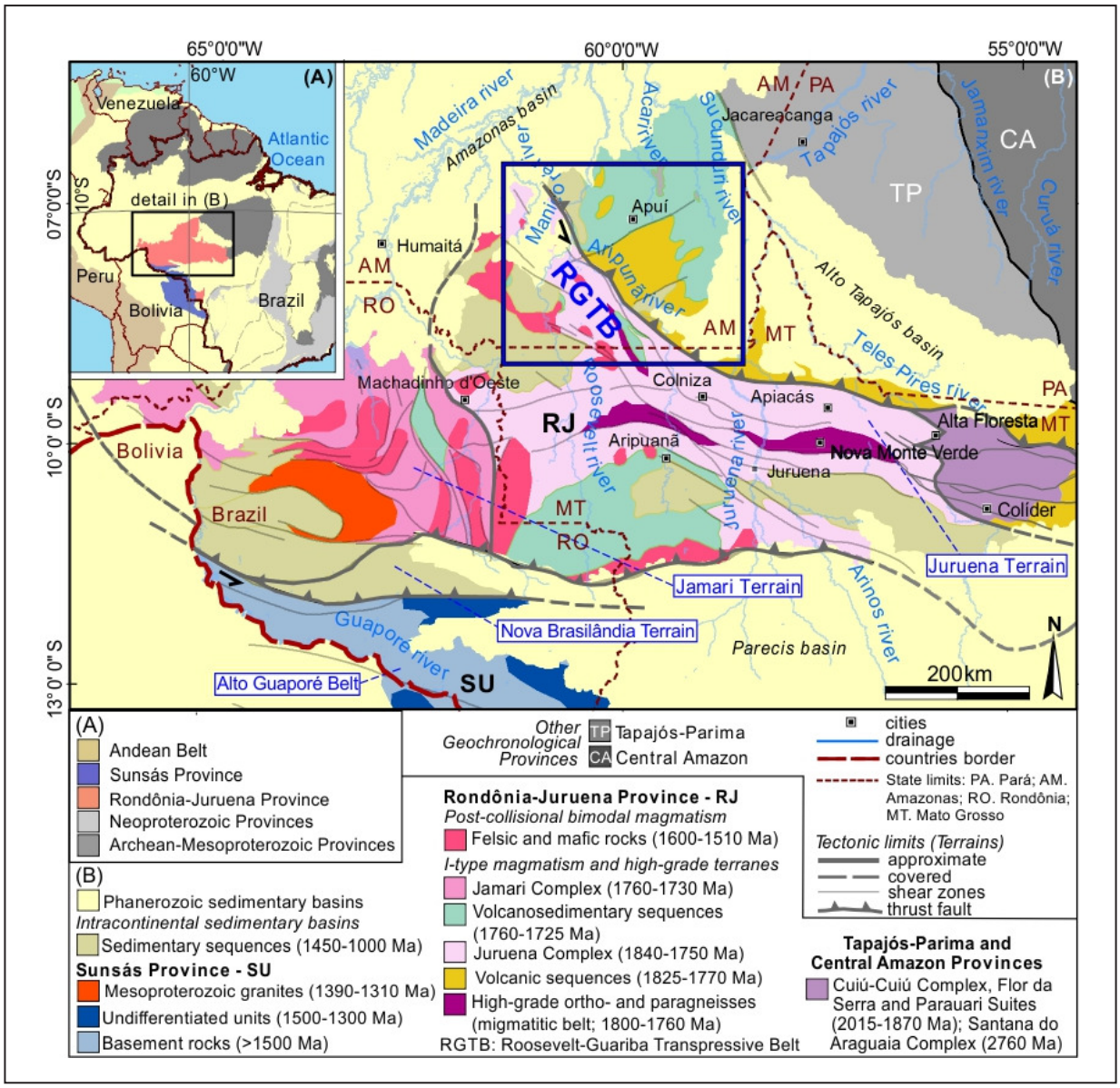

FIGURE 1. A) Map of the South American Platform highlighting the Rondônia-Juruena Province in the Amazon Craton (Santos et al. 2008); B) simplified geotectonic map of the Juruena Terrain according to Scandolara et al. (2016).

events and the tectonothermal effects in the Rondônia-Juruena Province. With this, the article intends to contribute also to the discussions about the configurations of supercontinent assemblies/break-ups in the southern region of the Amazon Craton and the involvement of the Juruena Terrain in the Columbia Supercontinent formation. In the Supercontinent cycle, separated blocks of continental crust can collide and merge, forming new and larger continents, triggering the tectonic framework of several orogenic belts, such Roosevelt-Guariba Transpressive Belt in the Juruena Terrain.

The understanding of the crustal growth/reworking may also help us to better define the crust architecture using isotopic mapping, constraining the distribution of mineral deposits. For example, BIF-hosted Fe deposits are spatially related to juvenile or reworked crustal domains and orogenic Au deposits are associated with juvenile crustal domains. In the specific case of the Juruena Terrain, the crust architecture is important to understand the chemical fertility and main structural footprints of the Au-(Cu) magmatic-hydrothermal deposits.

2. An overview of the Southeastern Amazonas geology: The Roosevelt-Guariba Transpressional Belt (RGTB) and surrounding areas

The studied area is located in the northern Juruena Terrain, forming the Rondônia-Juruena Province together with the Jamari and Jauru Terrains (1.82-1.54 Ga, Santos et al. 2008; Figure 1A,B). The Geochronological Province model for the Amazon Craton was originally based on Archean nuclei amalgamated through several accretionary and collisional

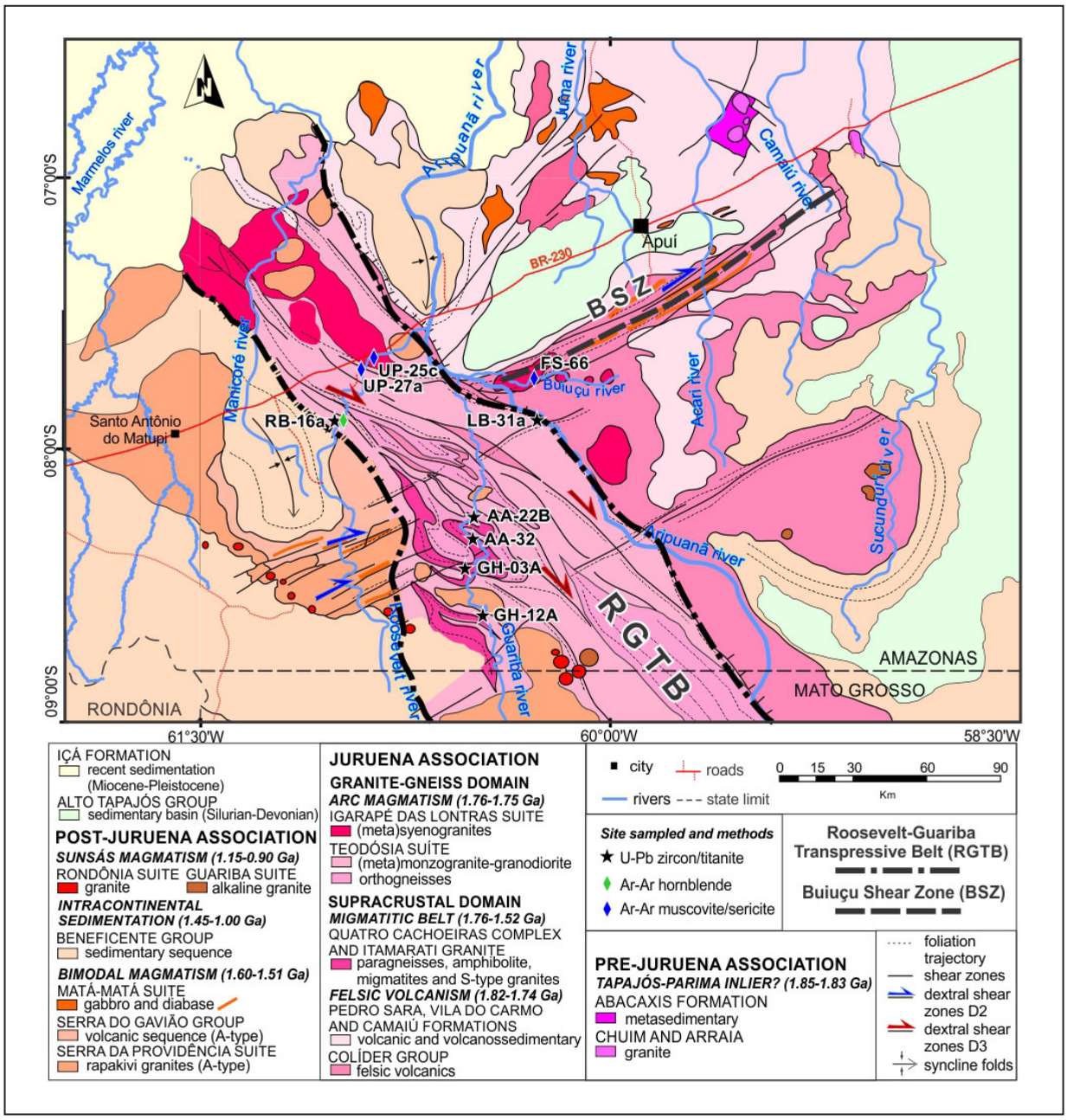

FIGURE 2. Simplified geological map of the North Juruena Terrain, Southeast of the Amazonas State (adapted from Reis et al. 2006, 2017; Almeida et al. 2016; Oliveira and Lira 2019; Meloni et al. 2021). Conventions: ATB – Alto Tapajós Basin; SD – Sucunduri Dome; MS – Machadinho Synclinal; JS – Jatuarana Synclinal; Au – gold occurrence.

Proterozoic terranes during Rhyacian to Tonian times (e.g. Amaral 1974; Cordani and Brito Neves 1982; Teixeira et al. 1989; Tassinari and Macambira 1999; Santos et al. 2000; Cordani and Teixeira 2007; Vasquez et al. 2008). However, multidisciplinary review studies at the regional scale show that province limits are not fully coincident with the geological and structural features (e.g. Scandolara et al. 2016; Roverato et al. 2017, 2019; Carneiro et al. 2018; Fernandes and Juliani 2019; Rizzotto 2019a, b; Oliveira and Almeida 2021; Trevisan et al. 2021; Motta et al. 2022; Almeida et al. 2022; Figure 1B).

Two main models have been proposed for the geodynamic evolution of the Juruena Terrain: i) accretionary evolution based on continental (e.g. Scandolara et al. 2016; Duarte et al. 2019) or island (Assis et al. 2017) magmatic arc systems; or ii) extensional within-plate or continental rifting settings (e.g. Neder et al. 2002; Barros et al. 2009; Rizzotto et al. 2019a, b). Alternative evolutionary models propose the alternation between compressive and extensional tectonic phases, responsible for crustal thickening and crustal thinning, respectively (Trevisan et al. 2021 and references therein).

Trevisan et al. (2021) identified three main magmatic events related to the crustal thickening and crustal thinning tectonic regimes in the Juruena Terrain, in response to flat and slab-rollback subduction, respectively. These magmatic events were defined by Alves et al. (2020) as (a) older continental magmatic arc with I-type calc-alkaline signature (Peixoto de Azevedo Domain: 2037- 1931 Ma), (b) magmatic arc in post-orogenic stage, with I-type calc-alkaline to alkali-calcic signatures (Juruena Supersuite: 1904–1851 Ma) and (c) intracontinental magmatism rift with A-type (locally I-type) alkali-calcic to alkaline signatures (Colíder Group and Teles Pires Suite: 1837–1757 Ma). This last event is associated to porphyry-type and epithermal mineralizations (Au-Cu-Mo, Cu-Mo e Au-Zn-Pb-Cu) in the Alta Floresta Mineral Province (Assis et al. 2017 and references therein).

In most evolutionary models, the geology and macrostructures of southeastern Amazonas are considered as being extensions of northeastern Rondônia and northern Mato Grosso (e.g. Trevisan et al. 2021 and references therein). However, recent works show that Northern Juruena Terrain (NJT) characteristics are contrasting with those existing in Rondônia and Mato Grosso, pointing to the predominance of well-preserved Sthaterian (volcano)sedimentary successions overlying an Orosirian basement with a crust having Tapajós-Parima age (Simões et al. 2020). Furthermore, the RGTB in southeastern Amazonas is oblique in relation to the regional WNW-ESE structures of the Juruena Complex in northern Mato Grosso (Ribeiro and Duarte 2010).

From multiscale regional studies and structural analysis, Oliveira and Almeida (2021) propose a tectonic compartmentalization for the NJT controlled by the RGTB. The RGTB is a high-T NW-SE-trend shear zone system with 60 km in width, cross-cutting the regional WNW-ESE structures of the Juruena Complex to the south. According to this compartmentalization, three petrotectonic associations are individualized: pre-Juruena, Juruena, and post-Juruena (Figure 2).

The Juruena Association is subdivided in two domains, the first (Supracrustal Domain) is located to the east, enclosing calc-alkaline to alkali-calcic volcanic rocks (I-type Colíder Group and A-type Pedro Sara Formation, 1820-1745 Ma; Duarte et al. 2019, Simões et al. 2020) and volcano-sedimentary successions (Camaiú Formation and Vila do Carmo Group, older than 1740 Ma). The tectonic setting is related to an intracontinental rift, similar to the other Sthatherian taphrogenetic systems observed in the Amazon, São Francisco-Congo and North China cratons, attributed to pre-breakup conditions of the Columbia Supercontinent (e.g. Reis et al. 2013; Simões et al. 2020). These supracrustal rocks show well-preserved subhorizontal primary structures, with the vertical tectonic locally exposing the basement through host-and-graben systems. This basement (pre-Juruena Association) is represented by the metavolcano-sedimentary succession with low metamorphic grade (Abacaxis Formation?), intruded by the Arraiá and Chuim granites (Matupi Suites, 1850–1835 Ma; Meloni et al. 2021).

According to Almeida et al. (2016) and Oliveira and Lira (2019), the second domain (Granite-Gneiss Domain) is formed by a high-temperature mylonitic belt (RGTB) showing igneous A-type to high-K calc-alkaline protoliths (Teodósia and Igarapé das Lontras Suites). Locally, paragneisses, amphibolites and migmatites (metavolcano-sedimentary succession of the Quatro Cachoeiras Complex) and deformed metavolcanic rocks (Colíder Group), metamorphosed under high-temperature upper amphibolite facies conditions and moderate pressure are described (Oliveira, 2016; Lisboa 2019).

The Supracrustal and Granite-Gneiss domains were tectonically juxtaposed as the consequence of the evolution of the RGTB (Oliveira and Almeida 2021). In southwest contact with the RGTB occurs bimodal magmatism represented by A2-type subalkaline rocks of the Serra da Providência Suite and Serra do Gavião Group, in association with tholeiitic gabbros and diabases related to the Post-Juruena Association. This southwest sector is characterized by a wide bimodal intracontinental post-orogenic magmatism (Scandolara et al. 2013) that locally intrudes the Granite-Gneiss and Supracrustal domains of the Juruena Association (e.g. Betiollo et al. 2009; Almeida et al. 2016; Meloni et al. 2021; Oliveira and Lira 2019).

Lastly, this terrain was recovered by younger and widespread intracratonic sedimentary sequences of the Manicoré, Prainha and Palmeiral formations, showing maximum sedimentation age around 1330-1100 Ma. According to Reis et al. (2013, 2017), this period represents the cratonization stage of the Juruena Terrain. These sedimentary sequences are delimited by normal faults produced from later reactivations of the RGTB, generating rollover structures and tilted blocks, as observed for example in the Jatuarana and Machadinho synclines (e.g. Almeida et al. 2016; Oliveira and Lira 2019).

3. Juruena Terrain: synthesis of previous geochronology data

The southeastern Amazonas is known for the scarcity of previous geochronological and isotopic data. The available data was mostly obtained during the seventies (Leal et al. 1978) using Rb/Sr and K/Ar methods (isochrone ages). Only recently, some new U-Pb and Sm-Nd data were published (e.g. Betiollo et al. 2009; Reis et al. 2013; Almeida et al. 2016). In contrast, the Rondônia-Juruena Province in the northeast Rondônia and northern Mato Grosso is better documented for geochronological data (e.g. Scandolara 2006; Scandolara et al. 2014, 2016; Duarte et al. 2012, 2019).

Abundant U-Pb zircon ages are available for widespread Paleoproterozoic calc-alkaline plutonism (Juruena Accretionary Belt; Scandolara et al., 2016) in northern Mato Grosso (e.g.

Pinho et al. 2003, Souza et al. 2005, Silva and Abram 2008, Ribeiro and Duarte 2010) and northeastern Rondônia (e.g. Scandolara 2006; Scandolara et al. 2014, Quadros et al. 2011). The main magmatic associations are represented by Paranaíta, Vitória, Vespor, São Pedro, São Romão suites, and Juruena Complex and orthoderived rocks of the Jamari Complex (Table 1; Figure 1), showing the main magmatic flare-up in the 1780-1760 Ma interval and magmatic lulls at 1860-1830 Ma (early stages) and 1720-1700 Ma (late stages).

The same is true for the U-Pb zircon ages of the corresponding volcanic rocks (Colíder Group and Pedro Sara Formation) of this magmatism in the Juruena Accretionary Belt. In northern Mato Grosso and southeastern Amazonas, the ages of the Colíder Group are for example as old as 1800 Ma (e.g. Pinho et al. 2003, Ribeiro and Duarte 2010, Almeida et al. 2016; Meloni et al. 2021), with at least ~60 Ma of duration (1820-1760 Ma; Table 1) and outcropping preferably around the Alto Tapajós Basin (Figure 2).

Also in northern Mato Grosso, some metavolcanic rocks (Roosevelt Group; Table 1) generated in an intermountain basin setting (rhyolites interbedded with clastic/chemical sediments) yielded a 1770-1740 interval age (e.g. Ribeiro and Duarte 2010; Neder et al. 2000; Santos et al., 2000). The Roosevelt Group, correlated with Vila do Carmo Basin located in southeastern Amazonas (Reis et al. 2013), was metamorphosed under greenschist to amphibolite facies conditions, with some retrograde metamorphism features. The main metamorphic event has 1652 ± 42 Ma (U/Pb SHRIMP, Pimentel, 2001) being of similar age as the observed in the deformed Moriru Volcanics (1662 ± 13 Ma; Pinho et al. 2003), contemporaneous with the Ouro Preto Orogeny (Santos et al. 2003).

The metavolcano-sedimentary rocks (Quatro Cachoeiras Complex; Table 1) in northeastern Rondônia were dated by Payolla et al. (2002, 2003a, b) and Quadros et al. (2011). The migmatitic metapelites yielded 1545-1542 Ma (zircon and monazite; U-Pb ID TIMS and U-Pb SHRIMP), interpreted as the main metamorphic (anatectic) event, coincident with the main phase of the Serra da Providência magmatic event (1.56-1.51 Ga). These rocks show also at least four inherited populations ages: (a) 1924 Ma; (b) 1868-1844 Ma; (c); 1805-1730 Ma (main) e (d) 1683-1662 Ma.

The two older populations are probably related to the Tapajós-Parima crust sources (2040-1860 Ma; Santos et al., 2000), while the main population shows strong relationships with source areas of the Juruena Accretionary Belt (1850-1730 Ma; Scandolara et al. 2016). The younger age population coincides with similar source areas of rocks of the Ouro Preto Orogeny (1670-1630 Ma; Santos et al., 2003). According to Payolla et al. (2002), the deposition of the Quatro Cachoeiras Basin had taken place between 1660 Ma and 1590 Ma (Table 1).

4. Geochronological results of Juruena Terrain in the Southeastern Amazonas

4.1. U-Pb SHRIMP and LA-ICP-MS results

4.1.1 Analytical procedures

In situ zircon U-Pb LA-ICP-MS (RB-16A sample, figure 3A; Table 2) analysis was carried out in the Laboratório de Estudos Geocronológicos, Geodinâmicos e Ambientais of the Universidade de Brasília (UnB), Brasília, Brazil, following all procedures described in Bühn et al. (2009). Concentrates of zircon were obtained by crushing the rock and then sieving and panning. Zircon crystals ranging from 0.177 mm (80#) to 0.074 mm (200#) were hand-picked under a binocular microscope, mounted in epoxy resin, and polished with diamond paste. The analyses were performed with a Thermo Finnigan Neptune multicollector inductively coupled plasma mass spectrometer with an attached New Wave 213μm Nd-YAG solid state laser, using a standard–sample bracketing technique with four sample analyses between a blank and a GJ-1 zircon standard. The accuracy was controlled using the zircon standard 91500. Ablation time and spot diameters were, respectively, 40 s and 30 mm for the U-Pb analyses. Raw data were reduced using an in-house program and corrections were done for background, instrumental mass-bias drift and common Pb, as described in Bühn et al. (2009). Analyses were preceded by backscattered electron (BSE) imagery also done at UnB using a Scanning Electron Microscope FEI Quanta 450.

Data were reduced using the SQUID© 1.02 software (Ludwig 2001) and the ages were calculated using Isoplot© 3.0 (Ludwig 2003). One determination on the standard was obtained for every three analyses of unknowns. Each spot size is typically 20-30 mm in diameter. The presented ages are mean average $^{207}Pb/^{206}Pb$ ages calculated at 2σ level, whereas the individual analyses are quoted at 1σ level.

Four samples (Table 2) of the Juruena Terrain are dated using U-Th-Pb SHRIMP (Sensitive High-Resolution Ion MicroProbe): mylonitic biotite granite (GH-03A, figure 3E), migmatitic paragneiss (AA-22B, figure 3G), amphibolite (AA-32, Figure 3H) and two-mica granodiorite (GH-12A, Figure 3F). Approximately 0.5 kg of each sample was collected and subsequently crushed, milled and sieved. The 60-200 mesh fractions were washed and dried to be processed using heavy liquids (LST-Lithium-Sodium-Tungstate and TBE-Tetra-Bromo-Ethane), which produced two fractions (lighter than 2.95 and heavier than 2.95). The heavy fraction was submitted to a hand magnet to remove fraction M1 (essentially magnetite and ilmenite). The fraction without magnetite was processed in a Frantz LB1 Isodynamic magnetic separator in two steps using an inclination of 18°. First, using 0.5 Ampère and 10° of lateral inclination and secondly using 1 ampere and 5 degrees of lateral inclination. This last step results in fractions M3 (where titanite was concentrated) and NM (where zircon was concentrated).

About 100 crystals of zircon were picked from the least magnetic fraction (NM) and – when present – about 20 crystals of titanite were picked from fraction M3. The selected grains were placed on double-sided tape together with fragments of standards. A cylinder measuring 25mm in internal diameter was placed on the double-sided tape and a liquid epoxy mixture was poured into it. The resulting epoxy disc was dried and polished using sandpaper and diamond paste of 1 micrometer. Each mount was initially carbon-coated to obtain backscattered electrons (BSE) images using a TESCAN-VEGA3 scanning electron microscope (SEM) at the Centre for Microscopy, Characterization, and Analysis, at the University of Western Australia. Images (BSE) were acquired under accelerating voltage of 20 kV, current of 10 nA, and a working distance of 15 mm. For the SHRIMP analyses, the mounts were lightly repolished and gold-coated. The isotopic U–Pb analyses were obtained at the SHRIMP II facilities of the Curtin

TABLE 1. Summary of main previous and new geochronological data of the Older basement (Pre-Juruena), Volcano-plutonic (Juruena), Supracrustal and Bimodal associations (Post-Juruena) in the Rondônia-Juruena Province. Abbreviations according to Siivola and Schmid (2007).

Sample	*rock*		*Metamorphism age (Ma)*	*M*	*Ref*	*Crystallization age (Ma)*	*Inherited/detrital age (Ma)*	*M*	*Ref*
			Pre-Juruena Associations						
I-type magmatism (Parauari/Matupá granites): 2000-1850 Ma									
Matupá Granite									
TRBY-20	Biotite syenogranite	N MT				1854 ± 8 zrn		E	Rocha et al. (2020)
n.a.	Biotite monzogranite	N MT				1869 ± 10 zrn		E	Silva et al. (2014)
n.a.	Granite	N MT				1872 ± 12 zrn		B	Moura (1998)
n.a.	Monzogranite	N MT				1872 ± 12 zrn		B	Moura (1998)
TRBY-27	Biotite syenogranite	N MT				1878 ± 8 zrn (autocryst)	1923 ± 17 zrn (antecryst)	E	Rocha et al. (2020)
n.a.	Biotite granite	N MT				1879 ± 5 zrn		D	Silva and Abram (2008)
n.a	Biotite granite	N MT				1889 ± 17 zrn		D	Silva and Abram (2008)
n.a.	Monzogranite	N MT				1894 ± 6 zrn		C	JICA; MMAJ (2000)
SD03	Porphyrytic granite (Aragão Granite)	N MT				1964 ± 11 zrn		E	Dezula et al. (2018)
SD05	Porphyrytic granite (Aragão Granite)	N MT				1967 ± 2 zrn		E	Dezula et al. (2018))
SD18	Inequigranular granite	N MT				1995 ± 5 zrn		E	Dezula et al. (2018)
n.a.	Biotite granodiorite	N MT				2001 ± 13 zrn		D	Silva et al. (2014)
SD20	Foliated granite	N MT				2009 ± 4 zrn		E	Dezula et al. (2018)
			Juruena Associations						
I- to A-type volcanic (Colíder Group and Sara Formation) and metavolcanic rocks (Roosevelt Group): 1825-1740 Ma									
Colíder Group									
FS-66A	Medium-grained ms-bearing phyllonite (Buiuçu River, Aripuanã River Basin)	SE AM	1300.1 ± 1.4 ms	A	This paper				
n.a.	Ignimbrite (Eastern Serra do Cachimbo)	N MT				1757 ± 14 zrn (autocryst)	1810 ± 14 zrn (antecryst)		Bini et al. (2015)
n.a.	Rhyolite	N MT				1766 ± 5 zrn		C	Souza et al. (2005)
B-04	Basalt (Moriru River, near Aripuanã City)	N MT				1764 ± 2 zrn (autocryst)	1776 ± 3 zrn (antecryst) 1780 ± 3 zrn (antecryst)	C	Pinho et al. (2003)
RB-12	Rhyolite	NE RO				1766 ± 5.7 zrn		D	Quadros and Rizzotto (2007)
n.a.	Ignimbrite	N MT				1770 ± 8 zrn		C	Souza et al. (2005)
B-01	Rhyolite (Moriru River, near Aripuanã City)	N MT				1770 ± 8 zrn		C	Pinho et al. (2003)
n.a.	Rhyolite (Gold Juma Garimpo)	SE AM				1770 ± 18 zrn		D	Brito et al. (2008)
SS-12	Crystal-rich lapilli tuff (Ema road, Apuí region)	SE AM				1781 ± 15 zrn		D	Meloni et al. (2021)
n.a.	na	N MT				1773 ± 5 zrn		C	Pimentel (2001)
WB-08	Rhyodacite ignimbritic (Moriru River, near Aripuanã City)	N MT				1774 ± 2 zrn		C	Pinho et al. (2003)
n.a.	Basalt	N MT				1776 ± 3 zrn		C	Souza et al. (2005)
B-03	Rhyodacite ignimbritic (Moriru River, near Aripuanã City)	N MT				1774 ± 10 zrn (autocryst)	1801 ± 11 zrn (antecryst)	C C	Pinho et al. (2003) Pinho et al. (2001)
GM-80	Porphyry rhyolite (SE Nova Santa Helena City, Vila Guarita Sheet)	N MT				1781 ± 8 zrn		C	Pimentel (2001)
MA-04	Porphyry rhyolite	N MT				1785 ± 6.3 zrn		D	Silva and Abram (2008)
TD-107	Andesite	N MT				1786 ± 12 zrn		D	Duarte (2015)
F2001	Porphyry rhyolite (NW Paranaíta City)	N MT				1786 ± 17 zrn		C	JICA; MMAJ (2000)
UP-43B	Breccia-like qtz trachyte (Branco Creek, Aripuanã River Basin)	SE AM				1791 ± 9.6 zrn		D	Almeida et al. (2016)

TABLE 1 (continuation)

Sample	*rock*		*Metamorphism age (Ma)*	*M*	*Ref*	*Crystallization age (Ma)*	*Inherited/detrital age (Ma)*	*M*	*Ref*
GM-08	Rhyolite	N MT				1792 ± 8 zrn		D	Alves et al. (2010)
n.a.	Ignimbrite (Guarantã do Norte region)	N MT				1792 ± 14 zrn		D	Silva et al. (2018)
FI-05	Mafic volcanic rock (Moriru River, near Aripuanã City)	N MT				1797 ± 5 zrn	1848 ± 9 zrn/ 1818 ± 9 zrn*	C C C*	Pinho et al. (2003) Pinho et al. (2001) Santos (2003)
TD-095	Rhyodacite	N MT				1803.5 ± 9.7 zrn		D	Duarte (2015)
LB-61	Rhyodacite (Buiuçu River, Aripuanã River Basin)	SE AM				1806 ± 8 zrn		E	Almeida et al. (2016)
n.a.	Rhyolite	N MT				1808±14 zrn		C	Souza et al. (2005)
DFR-14	Rhyolite (Lower sucession, Guarantã do Norte region)	N MT				1810 ± 9 zrn		D	Santos et al. (2019)
TL-144A	Porphyry dacite (Jatuarana Creek, Apuí region)	SE AM				1814 ± 9 zrn		D	Meloni et al. (2021)
TD-T-063K	Volcanoclastic rock	N MT				1820 ± 8 zrn		D	Duarte (2015)
n.a.	Felsic volcanic rock	SE AM				1825 ± 14 zrn		E	Reis et al. (2017)
Pedro Sara Formation									
RE-13B	Fenolatite (Acari River)	SE AM				1743.6 ± 7.5 zrn		D	Meloni et al. (2021)
SS-64B	Fenolatite (Acari River)	SE AM				1758 ± 12 zrn		D	Meloni et al. (2021)
RB-01	Acid volcanic rock	SE AM				1766 ± 5.7 zrn		D	Brito et al. (2010)
Roosevelt Group									
n.a.	Phylonite	N MT	1330 ± 6 ms	A					Silva and Abram (2008)
n.a.	Phylonite	N MT	1338 ± 7 ms	A					Silva and Abram (2008)
n.a.	Rhyolite	N MT				1730±9 zrn		D	Ribeiro and Duarte (2010)
MQ-96	Dacite (NE Rondônia and NW Mato Grosso border)	NE RO				1740 ± 8 zrn	1806 ± 11 zrn	E	Santos et al. (2000)
A-2	Mylonitic rhyodacite (high Aripuanã River)	N MT				1761 ± 5 zrn		C	Pinho et al. (2003)
01	Massaranduba Metadacite (Expedito Mine, NE Aripuanã City)	N MT				1762 ± 6 zrn		E	Neder et al. (2002)
n.a.	Dacite	N MT				1762 ± 6 zrn		D	Ribeiro and Duarte (2010)
A-1	Foliated rhyolite (high Aripuanã River)	N MT				1767 ± 2 zrn		C	Pinho et al. (2003)
PS-21	Metadacite	N MT				1772 ± 12 zrn		D	Ribeiro and Duarte (2010)
I-type hypabyssal granitoid rocks (Paranaíta Suite): 1816-1780 Ma									
GR-01A	Microgranite	N MT				1780.3 ± 4.5 zrn		D	Duarte (2015)
TD-T-050S	Porphyry granite	N MT				1790 ± 5.5 zrn		D	Duarte (2015)
n.a.	Hornblende-biotite porphyry syenogranite (Guarantã do Norte region)	N MT				1790 ± 6 zrn		D	Silva et al. (2018)
n.a.	Microgranular mafic enclave (Guarantã do Norte)	N MT				1790 ± 8 zrn		D	Silva et al. (2018)
n.a.	Monzogranite	N MT				1790 ± 6 zrn 1792 ± 5 zrn		E	Acevedo Serrato (2014)
CC-21	Biotite porphyry granite	N MT				1793 ± 6 zrn		C	Santos et al. (2000)
n.a.	Porphyry monzogranite (Guarantã do Norte region)	N MT				1794.4 ± 6.5 zrn		E	Silva et al. (2015)
n.a.	Hornblende-biotite porphyry syenogranite (Guarantã do Norte region)	N MT				1795± 6 zrn		D	Silva et al. (2018)

TABLE 1 (continuation)

Sample	*rock*		*Metamorphism age (Ma)*	*M*	*Ref*	*Crystallization age (Ma)*	*Inherited/detrital age (Ma)*	*M*	*Ref*
MC-120	Metamonzogranite	N MT				1796 ± 17		D	Duarte et al (2012)
TD-151	Porphyry syenogranite	N MT				1797 ± 14		D	Duarte et al (2012)
n.a.	n.a.	N MT				1801 ± 7 zrn		C	JICA; MMAJ (2000)
n.a.	Monzogranite	N MT				1803 ± 3 zrn		C	Pinho et al. (2003)
n.a.	n.a.	N MT				1803 ± 16 zrn		C	JICA; MMAJ (2000)
MA-12	Biotite granite	N MT				1808 ± 14 zrn		D	Silva and Abram (2008)
GR-01	Porphyry granite	N MT				1811 ± 6 zrn		D	Duarte (2015)
TD-T-050AM	Microgranite	N MT				1813.4 ± 5.1 zrn		D	Duarte (2015)
n.a.	n.a.	N MT				1816 ± 57 zrn		C	JICA; MMAJ (2000)
n.a.	Granite	N MT				1817 ± 6 zrn		C	JICA; MMAJ (2000)
n.a.	Granite	N MT				1819 ± 6 zrn		C	JICA; MMAJ (2000)
Orogenic I-type High-K calc-alkaline magmatism (Juruena and Jamari complexes, Vitória and Vespor suites, São Romão and São Pedro Granites): 1850-1730 Ma									
Vespor Suite									
MC-027Bb	Amphibolite	N MT	1439 ± 29 zrn	D	Duarte et al. (2012)				
n.a.	Tonalite	N MT				1750 ± 8 zrn		C	Pinho et al. (2003)
PS-29	Metagabbro	N MT				1764 ± 13 zrn		D	Ribeiro and Duarte (2010)
MC-31Bb	Metagabbro	N MT				1773 ± 15 zrn		D	Duarte et al. (2012)
São Pedro, São Romão, Peixoto de Azevedo and Nova Canaã Granites									
n.a.	Mylonitic leucogranite	N MT	1392 ms					A	Silva and Abram (2008)
P-18	Metagranodiorite	N MT	1669 ± 7 zrn	C	Pinho et al. (2003)				
n.a.	Metagranitoid	N MT	1652 ± 42 zrn	E	Pimentel et al. (2001)				
n.a.	Monzogranite	N MT				1721 zrn	1920 zrn	C	Leite et al. (2006)
n.a.	Syenogranite	N MT				1744 ± 15 zrn		C	Knust (2010)
A-6	Monzogranite gneiss (High Aripuanã River)	N MT				1759 ± 3 zrn		C	Pinho et al. (2003)
P-25	Biotite monzogranite gneiss	N MT				1763 ± 6 zrn		C	Pinho et al. (2003)
SK-55	Metamonzongranite	N MT				1763 ± 37 zrn		D	Knust (2010)
n.a.	Monzogranite	N MT				1764 ± 32 zrn		C	Pinho et al. (2003)
A-8	Hornblende Monzogranite (High Aripuanã River)	N MT				1766 ± 5 zrn		C	Pinho et al. (2003)
P-20	Syenogranite gneiss	N MT				1772 ± 4 zrn		C	Pinho et al. (2003)
JD-17B	Protomylonitic fine-grained biotite metagranite (São Romão type-area)	N MT				1770 ± 9 zrn		E	Souza et al. (2005)
A-3	Biotite monzogranite (High Aripuanã River)	N MT				1774 ± 4 zrn		C	Pinho et al. (2003)
PS-64	Metasyenogranite	N MT				1774 ± 28 zrn		D	Ribeiro and Duarte (2010)
n.a.	Monzogranite	N MT				1775 ± 13 zrn		C	Pinho et al. (2003)
WA-151	Metamonzogranite	N MT				1780 ± 13 zrn		C	Souza and Abreu (2007)

TABLE 1 (continuation)

Sample	*rock*		*Metamorphism age (Ma)*	*M*	*Ref*	*Crystallization age (Ma)*	*Inherited/detrital age (Ma)*	*M*	*Ref*
FR-02	Biotite granodiorite	N MT				1781 ± 10 zrn		E	Silva et al. (2014)
CC158	Metamonzogranite	N MT				1784 ± 17 zrn		E	Souza et al. (2005)
CC138	Garnet-biotite metagranite	N MT				1786 ± 17 zrn		E	Santos et al. (2004)
A-7	Hornblende monzogranite (High Aripuanã River)	N MT				1799 ± 15 zrn		C	Pinho et al. (2003)
P-29	Weathered monzogranite (Colniza-Mina Bzrn Aripuanã Road)	N MT				1803 ± 2 zrn		C	Pinho et al. (2003)
n.a.	Quartz monzonite	N MT				1798±14 zrn		D	Silva and Abram (2008)
Vitória Suite									
P-21	Foliated granodiorite (Colniza-Mina Bzrn Aripuanã Road)	N MT				1765 ± 4 zrn		C	Pinho et al. (2003)
WA-227A	Tonalite	N MT				1771 ± 14 zrn		D	Souza and Abreu (2007)
CC233	Enderbite	N MT				1775 ± 10 zrn	1879 zrn	E	Souza et al. (2005)
MC-027Aa	Metatonalite	N MT				1783 ± 14 zrn		D	Duarte et al. (2012)
PS42	Tonalite	N MT				1785 ± 8 zrn		E	Souza et al. (2005)
PS306	Metagranodiorite	N MT				1785 ± 8 zrn		D	Ribeiro and Duarte (2010)
Jamari Complex									
PG-JS-26	Tonalite gneiss	NE RO				1728 ± 15 zrn		E	Silva et al. (2002)
PS-19	Metamonzogranite	NE RO				1730 ± 9 zrn		D	Ribeiro and Duarte (2010)
WB-70	Enderbitic granulite	NE RO				1730 ± 22 zrn		C	Payolla et al. (2002)
JL-78	Tonalite	NE RO	1334 ± 7 zrn	E	Santos et al. (2008)	1738 ± 6 zrn		E	Santos et al. (2008)
GR-59	Tonalite	NE RO	1677 ± 6 zrn	E	Santos et al. (2008)	1753 ± 9 zrn		E	Santos et al. (2008)
GR-35	Quartz diorite	NE RO				1758 ± 7 zrn		E	Santos et al. (2008)
LP-122	Metatonalite (Cujubim region)	NE RO				1758.7 ± 4.1 zrn		D	Quadros et al. (2011)
Juruena Complex?									
n.a.	n.a.	N MT				1806 ± 3 zrn		E	Santos (2003)
n.a.	n.a. (Vila Guarita region)	N MT				1817 ± 57 zrn		C	JICA/MMAJ (2000)
n.a.	n.a. (Vila Guarita region)	N MT				1823 ± 35 zrn		C	JICA/MMAJ (2000)
n.a.	n.a. (Vila Guarita region)	N MT				1848 ± 17 zrn		C	JICA/MMAJ (2000)
Orogenic High-K calc-alkaline magmatism HFSE-enriched (Teodósia Suite): 1758-1749 Ma									
GH-03A	Mylonitic bt granite (Guariba River, Aripuanã River basin)	SE AM				1749 ± 10 zrn, ttn		E	This paper
LB-31A	Hbl-bt monzogranite (Teodósia falls, type-area, Aripuanã River)	SE AM				1754 ± 8 zrn		C	Mod. Almeida et al. (2009)
Late-orogenic Transitional I-A-type (Igarapé das Lontras Suite):1754-1736									
UP-25C	Fine-grained se-bearing phyllonite (Roosevelt River, Aripuanã River Basin)	SE AM	1466.5 ± 1.4 ser	A	This paper				
UP-27A	Medium-grained op-ms-qtz phyllonite (Roosevelt River, Aripuanã River basin)	SE AM	1467.6 ± 0.8 ms	A	This paper				
RB-16A	hbl-bt augen gneiss/high-T mylonite (Roosevelt River, Aripuanã River basin)	SE AM	1482.9 ± 1.3 hbl	A	This paper	1736 ± 29 zrn (autocryst)	1764 ± 13 zrn (antecryst) 1807 ± 47 zrn 1877 ± 44 zrn	E	mod. Almeida et al. (2009)

TABLE 1 (continuation)

Sample	*rock*		*Metamorphism age (Ma)*	*M*	*Ref*	*Crystallization age (Ma)*	*Inherited/detrital age (Ma)*	*M*	*Ref*
LB-73B	Ep-bt-ms metarhyolite (Buiuçu River, Aripuanã River Basin)	SE AM				1754 ± 6 zrn (autocryst)	1798 ± 8 zrn (antecryst)	E	Almeida et al. (2016)
LB-68	Protocataclastic leucomicrosyenogranite (Buiuçu River, Aripuanã River Basin)	SE AM				?	1790 ± 18 zrn	D	Almeida et al. (2016)
Late-orogenic Transitional I-A-type (Teles Pires Suite):1754-1736									
n.a.	Zé do Torno Granite	N MT				1743 ± 4 zrn		E	Frasca and Borges (2004)
02	Paraibão Granite (Expedito Mine, NE Aripuanã City)	N MT				1755 ± 5 zrn		E	Neder et al. (2002)
GM-10	Biotite granite (SE Terra Nova do Norte City)	N MT				1757 ± 16 zrn		C	Pimentel (2001)
n.a.	Syenogranite (Guarantã do Norte region)	N MT				1763 ± 14 znr	1811 ± 15 zrn	D	Silva et al. (2018)
n.a.	Monzogranite	N MT				1760 ± 12 zrn		C	Silva and Abram (2008)
n.a.	Leucogranite	N MT				1782 ± 17 zrn		D	Silva and Abram (2008)
n.a.	Granite	N MT				1727 ± 42 zrn		D	Prado et al. (2013)
			Post-Juruena Associations						
High grade Paragneiss Sucessions and S-type Granites: 1660-1590 Ma (deposition) and 1545-1520 Ma (anatexis)									
Quatro Cachoeiras Complex and Itamaraty Suite									
WB-152	High-grade metapelite migmatitic (Oriente Novo region, Machadinho River basin)	NE RO	1454 zrn 1545-1524 zrn 1589 zrn	E	Payolla et al. (2003a)		1662 zrn (detrital?) 1805-1769 zrn 1868-1844 zrn 1924 zrn	E	Payolla et al. (2003a)
			1544.6 ± 3.7 mnz		Payolla et al. (2003b)				
JWB-24/A	Metapelitic migmatite (Oriente Novo region, Machadinho River basin)	NE RO	1384 zrn 1590 zrn	E	Payolla et al. (2003a)		1730 zrn 1797 zrn	E	Payolla et al. (2003a)
WB-142	Metapelitic migmatite (Jaru region, Jamari River basin)	NE RO	1542 ± 3.5 mnz	E	Payolla et al. (2003b)				
AA-22B	Migmatitic paragneis/mesossome (Guariba River)	SE AM	1526 ± 5 zrn	E	This paper				
AA-32	Amphibolite (Guariba River)	SE AM				1752 ± 6 zrn		E	This paper
GH-12A	Two-mica granodiorite (Guariba River)	SE AM				1520 ± 12 zrn	1790 ± 6 zrn 1839 ± 22 zrn	E	This paper
LP-133	Peraluminous metagranitoid (Machadinho River basin)	NE RO				1553 ± 20 zrn		D	Quadros et al. (2011)
Bimodal Magmatism A-type rapakivi (Serra da Providência Suite) and gabbroic-diabase rocks (Mata-Matá Diabase): 1600-1500 Ma									
Serra da Providência Suite									
AC-08D	Alkalifeldspar microgranite with hematite and fluorite (Roosevelt River, Amazonas)	SE AM				1503 ± 24 zrn		E	Oliveira and Lira (2019)
GH-11	Arf-bt quartz syenite (Guariba River, Amazonas)	SE AM				1511 ± 8.4 zrn		D	Oliveira and Lira (2019)
GR-333	Metagranite	NE RO				1515 ± 8 zrn		E	Santos et al. (2008)
AC-23A	Fl syenogranite (Roosevelt River, Amazonas)	SE AM				1516 ± 3.8 zrn		D	Oliveira and Lira (2019)
PS-170	Hbl-bt syenogranite (Rio Guariba Sheet, Mato Grosso)	N MT				1516 ± 13 zrn 1505 ± 9.8 tt		D	Ribeiro and Duarte (2010)
n.a.	Hbl-bt syenogranite	N MT				1516 ± 11 zrn		D	Ribeiro and Duarte (2010)
n.a.	Monzogranite	SE AM				1520±12 zrn	1804±16 zrn	E	Oliveira and Lira (2019)
PG-JS-32	Monzogranitic gneiss	N MT				1522 ± 10 zrn		E	Silva et al. (2002)

TABLE 1 (continuation)

Sample	*rock*		*Metamorphism age (Ma)*	*M*	*Ref*	*Crystallization age (Ma)*	*Inherited/detrital age (Ma)*	*M*	*Ref*
WB-44ª	Syenogranitic gneiss	NE RO				1526 ± 12 zrn		C	Payolla et al. (2002)
n.a.	Granite (União Massif, Rondônia)	NE RO				1526 ± 12 zrn		D	Payolla et al. (1998)
AC-08A	Ignimbrite rhyolitic with fluorite (Roosevelt River, Amazonas)	SE AM				1529.7 ± 5.5 zrn		E	Oliveira and Lira (2019)
WB-36	Quartz syenite	NE RO				1532 zrn		C	Payolla et al. (2002)
n.a.	Quartz syenite (União Massif, Rondônia)	NE RO				1532 ± 5 zrn		C	Bittencourt et al. (1999)
FS-30A	Wiborgite (Vila Maravilha Granite, Amazonas) Xenolith (piroxene granodiorite gneiss)	SE AM	1576 ± 13 zrn	B	Almeida et al. (2016)	1534 ± 4 zrn 1715 ± 8 zrn		B	Almeida et al. (2016)
PG-JS-01	Monzogranitic gneiss	N MT				1535 ± 27 zrn		E	Silva et al. (2002)
MA-04	Porphyry dacite (Guariba River mouth, Amazonas)	SE AM				1536 ± 2 zrn	1750 zrn 1775 zrn	B	Almeida et al. (2016)
LP-81	Mylonitc meta monzogranite (Aquariquara Massif, Rondônia, LH C-70)	NE RO				1536 ± 22 zrn		D	Quadros et al. (2011)
MQ-33	Ttn-bt monzogranite	NE RO				1537 ± 7 zrn		C	Rizzotto et al. (2002)
n.a.	Porphyrytic biotite syenogranite (Aripuanã Granite, Mato Grosso)	NE RO				1546 ± 5 zrn 1537 ± 7 zrn		B D	Rizzotto et al. (2002)
AR-3/1	Monzogranite	NE RO				1544 ± 5 zrn		C	Payolla et al. (2002)
PG-JS-19	Syenogranitic gneiss	N MT				1545 ± 8 zrn		E	Silva et al. (2002)
LP-42	Charnockite (União Massif, Rondônia, Gramazon mine, Rondônia)	NE RO				1547 +19/-9 zrn		D	Quadros et al. (2011)
n.a.	Protomylonitic syenogranite	NE RO				1552 ± 4 zrn		B	Rizzotto et al. (2006)
SK-71	Charnockite (Rio Guariba Sheet, Mato Grosso)	N MT				1552 ± 7 zrn	1890 zrn	D	Ribeiro and Duarte (2010)
SP-GR-53	Syenogranite	NE RO				1554 ± 47 zrn		C	Bettencourt et al. (1999)
PG-JS-16	Monzogranitic gneiss	N MT				1555 ± 19 zrn		E	Silva et al. (2002)
n.a.	Monzogranite	N MT				1557±13 zrn		D	**Souza and Abreu (2007)**
RE-111A	Meta syenogranite (Aquariquara Massif, Rondônia, LH C-66)	NE RO				1557 ± 17 zrn		D	Quadros et al. (2011)
n.a.	Chanockite (Jaru Charnockite, Rondônia)	NE RO				1559 zrn		D	Payolla et al. (1998)
WA-46A/C	Monzogranitic gneiss	NE RO				1560 zrn		C	Payolla et al. (2002)
WA-45	Granodiorite	N MT				1564 ± 12 zrn		C	Souza and Abreu (2007)
SP-GR-48	Wiborgite	NE RO				1566 ± 3 zrn		C	Bettencourt et al. (1999)
SP-GR-39	Piterlite	NE RO				1566 ± 5 zrn		C	Bettencourt et al. (1999)
WO-63	Augen gneiss (Ouro Preto D´Oeste, Rondônia)	NE RO				1569 ± 18 zrn		D	Santos et al. (2000)
SP-GR-21	Hbl-bt monzogranite	NE RO				1573 ± 15 zrn		C	Bettencourt et al. (1999)
MS-6030	Granitic gneiss	NE RO				1570 ± 15 zrn		C	Payolla et al. (2002)
GR-48	Granitic gneiss	NE RO				1570 ± 17 zrn		E	Bettencourt et al. (1999)
GM-33	Mylonitic granite	N MT				1580 ± 35 zrn		C	Martins and Abdallah (2007)
SP-GR-76	Porphyritic bt syenogranite	NE RO				1606 ± 24 zrn		C	Bettencourt et al. (1999)

TABLE 1 (continuation)

Sample	*rock*		*Metamorphism age (Ma)*	*M*	*Ref*	*Crystallization age (Ma)*	*Inherited/detrital age (Ma)*	*M*	*Ref*
Mata-Matá Mafic Rocks									
AC-15B	Foliated metadiabase (Roosevelt River, Amazonas)	SE AM				1529 ± 21 zrn	1877 ± 13 zrn 1954 ± 22 zrn 1799 ± 22 zrn	E	Oliveira and Lira (2019)
AC-16A	Foliated metadiabase (Roosevelt River, Amazonas)	SE AM					1847 ± 19 zrn 1889 ± 18 zrn 2026 ± 18 zrn	E	Oliveira and Lira (2019)
LB-19D	Olivine gabbro	SE AM				1540 bdy		E	Almeida et al. (2016)
RE-03	Olivine gabbro (Domingas Gabbro, Juma mine, Amazonas)	SE AM				1552 ± 7 bdy		D	Meloni et al. (2021)
LB-02C2	Olivine gabbro (Matá-Matá Gabbro, Aripuanã River, Amazonas)	SE AM				1576 ± 4 bdy		E	Betiollo et al. (2009)

A. Ar-Ar step heating; B. Pb-Pb zircon evaporation; C. U-Pb ID TIMS; D. U-Pb ICP-MS-LA; E. U-Pb SHRIMP. Abbreviations: n.a. not avaliable. Region: SE AM. Southeastern Amazonas; NE RO. Northeastern Rondônia; N MT. Northern Mato Grosso. Minerals: zrn. Zircon; mnz. Monazite; ttn. Titanite; mnz. Monazite; hbl. Hornblende; ser. Sericite; ms. Muscovite. Terminologies according Miller et al. (2007): 1. Antecrysts: zircon grains that crystallized from earlier pulses (a crystal from an earlier pulse of magma which is incorporated by later pulses); 2. Autocrysts: grains generated within the youngest intrusive pulse (spatially and temporally associated with a distinct pulse or increment of magma); 3. Xenocrysts: grains assimilated from host rocks sufficiently older (at least several million years), being considered unrelated to the magma system; 4. Inherited: grain that comes from the melt source.

TABLE 2. Simplified description and location of the dated samples, including summary of ages and methods. Abbreviations according Siivola and Schmid (2007).

sample	*stratigraphic unit*	*Coord.*	*sample description*	*Ages (Ma)*	*Method*
RB-16A	Igarapé das Lontras Suite (Roosevelt River)	-7.92105 -60.98940	Hbl-bt augen gneiss (high-T mylonite) with coarse to medium grained groundmass and ovoid afs megacrystals (<6 cm). Accessory minerals: ttn, mag, ep, ap. (figure 3A)	1483 ± 1 1877 ± 44 1807 ± 47 1764 ± 13 1736 ± 29	hbl Ar-Ar step heating zrn U-Pb LA-ICP-MS
GH-03A	Teodósia Suite (Guariba River)	-8.48162 -60.51497	Mylonitic bt granite, pale-pinked, medium-grained recrystallized (moderate) groundmass with aln, ep, ttn, hbl, ap and zrn, and centimetric rounded fsp porphyroclasts (figure 3E)	1749 ± 10	zrn, ttn U-Pb SHRIMP
LB-31A	Teodósia Suite (Aripuanã River, type-area)	-7.86370 -60.26528	Equigranular, pale gray, medium-grained hbl-bt monzogranite, with subrounded/irregular mafic clots. Accessory minerals: ttn, ep, mag, ap, zrn (figure 3B)	1754 ± 8	zrn U-Pb SHRIMP
AA-22B	Quatro Cachoeiras Complex (Guariba River)	-8.28286 -60.48390	Migmatitic ms-bt paragneiss, medium-grained, stromatic and polifolded, with crd, and, op. (figure 3G)	1752 ± 6 1526 ± 5	zrn U-Pb SHRIMP
AA-32	Quatro Cachoeiras Complex (Guariba River)	-8.40886 -60.49350	Fine-grained amphibolite with pgo, hbl, bt, rarely aug (igneous relict), further op, zi and ap. (figure 3H)	1762 ± 7	
GH-12A	Itamarati Suite (Guariba River)	-8.62759 -60.45697	Foliated two-mica granodiorite, pale-gray, equigranular, medium-grained, with and, sil, chl. (figure 3F)	1805 ± 13 1520 ± 12	
UP-25C	Igarapé das Lontras Suite (Roosevelt River)	-7.16028 60.68532	Fine-grained phyllonite, resembling a se-qtz schist (mylonitic metamicrogranite altered and strongly deformed), with S-C foliations, mica fish and qtz porphyroclasts (65%)(figure 3D)	1467 ± 1	se Ar-Ar step heating
UP-27A	Igarapé das Lontras Suite (Roosevelt River)	-7.20369 -60.65157	Medium-grained phyllonite with op (5%), macroscopically resembling a ms-qtz-bt-schist, equi-granular with granolepidoblastic texture and lenses of qtz aggregates. (figure 3C)	1468 ± 1	ms Ar-Ar step heating
FS-66A	Colíder Group (Buiuçu River)	-7.75252 -60.26949	Medium-grained phyllonite (ms-bearing afs-qtz-phyllite), corresponding to sheared felsic hypoabissal rock, with ms (45%), qtz (50%), as policrystalline aggregates with undolose extinction, and afs (5%) porphyroclasts (anhedral shapes/granoblastic textures)	1300 ± 1	

University of Technology in Perth, Western Australia, following the procedures described by Compston et al. (1984, 1992) and the operational routine described by Smith et al. (1998). Individual analyses are composed of nine measurements for zircon ($^{196}Zr_2O$, ^{204}Pb, background, ^{206}Pb, ^{207}Pb, ^{208}Pb, ^{238}U, ^{248}ThO, ^{254}UO), and nine measurements for titanite (^{200}Ti-Ca peak, ^{204}Pb, background, ^{206}Pb, ^{207}Pb, ^{208}Pb, ^{248}ThO, ^{254}UO, and $^{270}UO_2$) repeated in five scans. The standards zircon D23 and glass NBS611 were used to identify the position of the peak of mass ^{204}Pb, whereas the calibration of the U content and the Pb/U ratio was done using the zircon standard BR266 (559 Ma, 903 ppm U; Stern 2001) and titanite standard Khan (522 Ma; 680 ppm U; Heaman 2009).

4.1.2 High-K calc-alkaline (I type to transitional I/A-type) deformed granitoids (Igarapé das Lontras and Teodósia Suites)

The isotopic dataset of Almeida et al. (2009) was revised, considering the hornblende-biotite augen gneiss (RB-16A sample) located in the Roosevelt River (Table 2; Figures 2 and 3A). These authors obtained previously a crystallization age of 1758.2 ± 4.7 Ma, interpreted as that of the protolith of the São Romão Suite (I-type Andean-type magmatism). However, Almeida et al. (2016) point to an A-type chemical signature for this sample, contrasting with a calc-alkaline trend.

A more detailed review of this isotopic data shows at least four age populations with low Th/U ratios (0.4-0.2, locally 0.7-0.6), despite some age overlaps occurring within analytical error (Table 3; Figure 4A): i) 1877 ± 44 Ma; ii) 1807 ± 47 Ma; iii) 1764 ± 13 Ma; and iv) 1736 ± 29 Ma. The older age (1877 Ma) was obtained from two inherited crystals (upper intercept), attributed to rocks with Silicic Large Igneous Province (SLIP) Uatumã age (Tapajós-Parima crust; see Klein et al. 2012). Two other crystals yielded an age of 1807 ± 47 Ma (upper intercept), probably related to the early stages of the Accretionary Juruena Belt. However, within error margin, these apparent two populations may be only one, recording, together, the origin of the Accretionary Juruena Belt.

The main population (15 crystals) yielded an age of 1764 ± 13 Ma (antecrysts in the sense of Miller et al. 2007), corresponding to grains generated within the earlier magmatic pulses, which the zircon crystals are normally greater (100-370 µm) and brighter in BSE images, showing also well-defined magmatic zoning (Figure 5A, e.g. Z9, Z13, Z17, Z19 and Z22 crystals). In turn, these antecrysts are incorporated by later pulses, represented by the younger population of 1736 ± 29 Ma (concordia age), interpreted as the crystallization age of the protolith. Thus, both zircon populations were generated in the same magmatic event and the protolith is a granitoid rock of the Igarapé das Lontras Suite, correlated in age to the Jamari Complex (1.76-1.73 Ga; Table 1, Figure 1).

Two other samples belonging to the Juruena Accretionary Belt were also analyzed. The LB-31A sample (Table 2; Figures 2 and 3B) comes from the type area of the Teodósia Suite, Aripuanã River, representing a rare undeformed granitic rock. Ten zircon crystals yielded a Concordia age of 1754 ± 8 Ma (Table 3; Figure 4B), in accordance with Almeida et al. (2005) original results (Table 2), showing high Th/U ratios (1.1-0.6). The zircon crystals are fractured, showing corroded edges, apatite inclusions and slight magmatic zoning (Figure 5B, C). In the Guariba River (Figure 1), a well-foliated (NW-trending) mylonitic biotite granite (GH-03A; Table 2; Figures 2 and 3E) yielded a concordant age of 1749 ± 10 Ma (Table 3; Figure 4C) from seven zircons and three titanites, interpreted as the crystallization age of the protolith. The colorless to pale yellow zircon crystals are euhedral, bipyramidal, and show magmatic zoning and high Th/U ratios (1.6-1.0), with no inherited cores and inclusions. Titanites are also typically igneous (Figure 5D) showing 0.9-0.8 Th/U ratios.

4.1.3 High grade supracrustal rocks (Quatro Cachoeiras Complex)

Migmatitic paragneisses (AA-22B) and amphibolites (AA-32) metamorphosed in high-grade conditions, restricted to the middle course of the Guariba river (Table 2; Figures 2 and 3G,H), were selected for zircon U-Pb SHRIMP analysis (Table 3; Figure 4D). These rocks were correlated to the Quatro Cachoeiras Complex, described in the northeastern of Rondônia (Quadros et al. 2011), located about 100 km to the west of study area.

The migmatitic paragneiss (AA-22B) is stromatic, poli-folded, showing NW-trending main foliation and two different zircon ages (Figures 4D and 5E, F). The younger age was obtained from five zircon crystals. yielding a concordant age of 1526.1 ± 4.6 Ma (MSWD = 7.0), with lower Th/U ratio (0.7-0.5), interpreted as the main anatectic/migmatization event. An older concordant age of 1752.0 ± 5.7 Ma was recorded based on four zircon crystals (MSWD = 3.9), showing higher Th/U ratios (0.8-0.7), considered as inherited ages derived probably derived from the calc-alkaline basement rocks (Teodósia Suite?).

The amphibolite (AA-32) occurs as rotated boudins in the paraderived succession and yielded a concordant age of 1762.2 ± 6.7 Ma (MSWD = 1.8) from nine zircon crystals (Figure 4E), showing wide Th/U variation (0.7-0.01). This age testifies to a contemporaneity between the mafic magmatism of the Quatro Cachoeiras basin and the calc-alkaline magmatism generated in the late stages (1.76-1.74 Ga) of the Juruena Accretionary Belt.

In the northeastern of Rondônia, the metapelitic migmatites of the Quatro Cachoeiras Complex yielded strongly variable inherited ages suggesting wide zircon provenance and metamorphic age (Payolla et al. 2002, 2003a, b; Quadros et al. 2011). Based on U-Pb ID TIMS (monazite) and U-Pb SHRIMP (zircon) analysis, Payolla et al. (2003a, b) determined metamorphic ages with intervals varying from 1545-1542 Ma (monazite) to 1590-1524 Ma (1545 ± 8 Ma in average; zircon), suggesting a Calymmian anatectic event in the Rondônia-Juruena Province. The zircon inherited ages show a more diversified spectrum when compared to the paragnaisses of the Guariba River: (a) 1924 Ma; (b) 1868-1844 Ma; (c); 1805-1730 Ma (main population) e (d) 1683-1662 Ma.

4.1.4 Peraluminous two-mica granite (Itamarati Suite)

In the Guariba River (Figure 2), small bodies (1m to <2 km) of peraluminous S-type biotite-muscovite granites (GH-12A; Figure 3F) show two different age zircon populations (Table 3; Figure 4F): (a) concordant age of 1520 ± 12 Ma (only one zircon crystal; Figure 5H) with low Th/U ratio (0.4); (b) concordant age of 1805 ± 13 Ma (eight zircon crystals and MSWD = 4.2; Figure 5G,I) and high Th/U ratios (1.1-0.6). The younger age (c. 1520

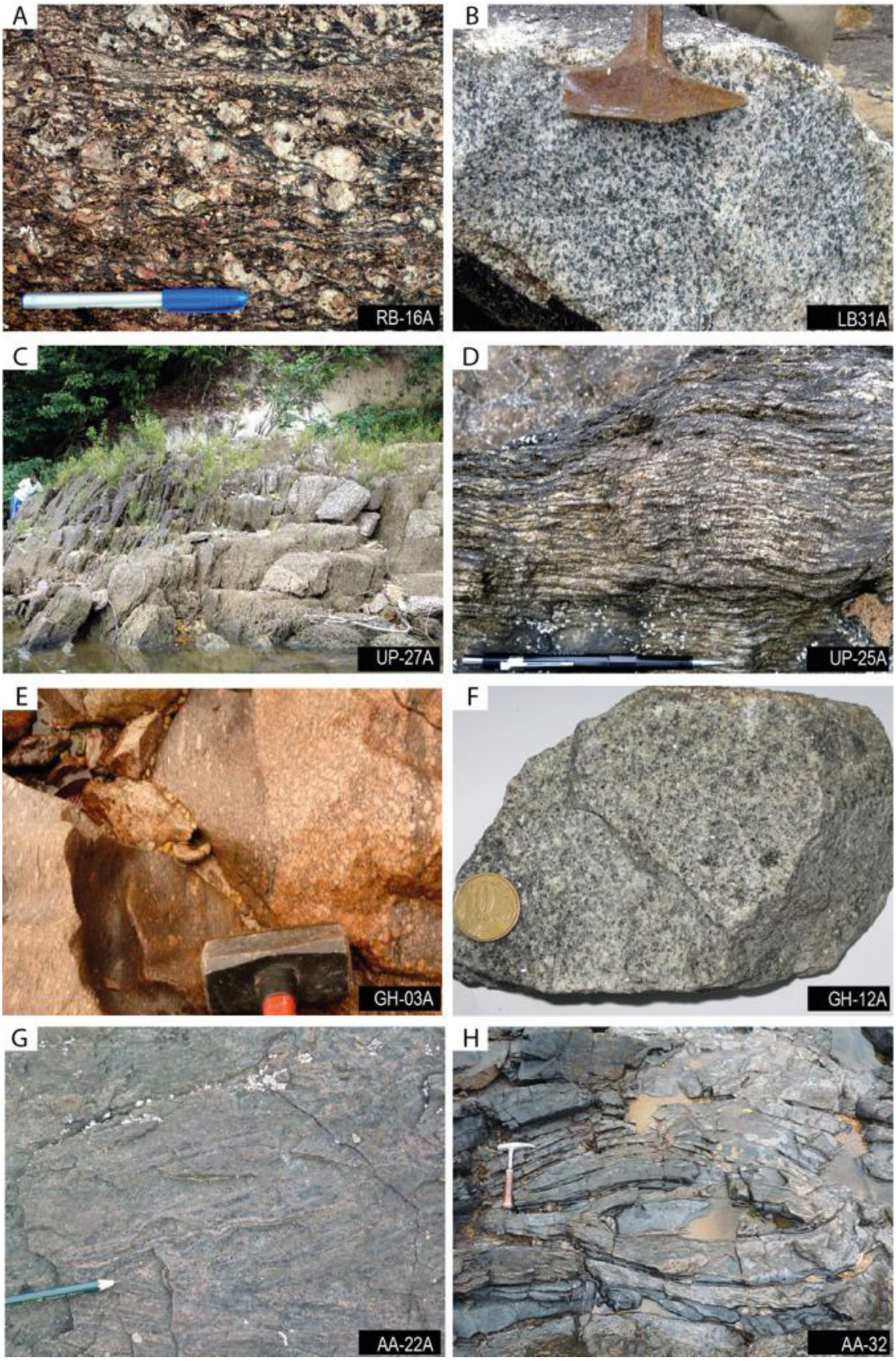

FIGURE 3. Field and textural characteristics of the Juruena rocks in RGTB, submitted to geochronological analysis, represented by Granite-gneiss Domain: (A) augen gneiss, (B) isotropic granites, (C,D) phyllonites, (E) foliated granitoids; and Supracrustal Domain: (F) S-type leucogranites, (G) stromatic metatexite leucosome rich (migmatite paragnaisses) and (H) amphibolites.

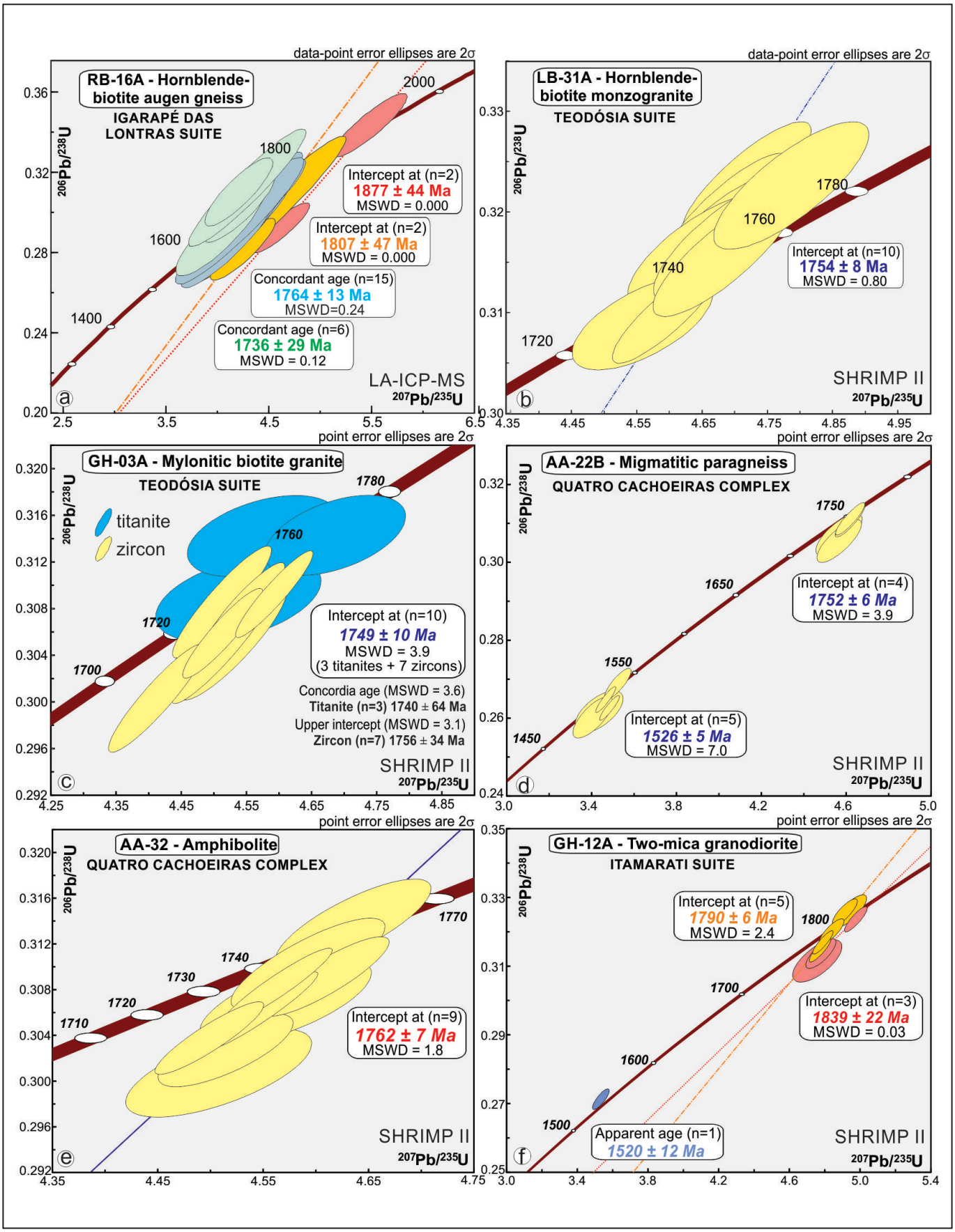

FIGURE 4. U–Pb concordia diagrams of U-Pb data on zircon and titanite from analyzed samples: A. Augen gneiss (RB-16A); B. Monzogranite (LB-31A); C. Mylonitic biotite granite (GH-03A); D. Migmatitic paragneiss (AA-22B); E. Amphibolite (AA-32); and F. Two-mica granodiorite (GH-12A).

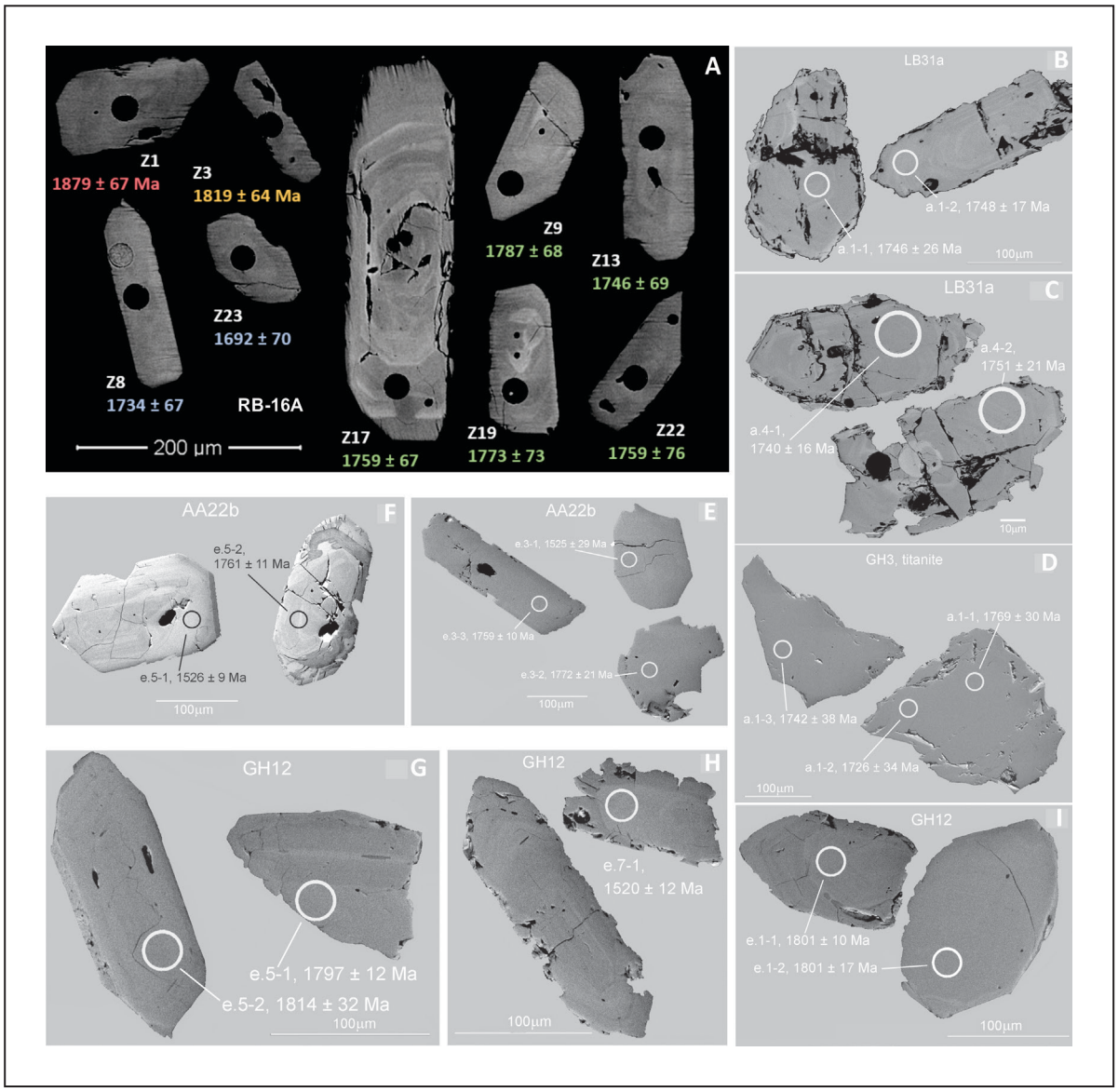

FIGURE 5. Examples of back-scattered electrons (BSE) images of the analysed zircons: A. RB-16A; B,C. LB-31A; D. GH-03A; E,F. AA-22B; and G,H,I. GH-12A.

Ma) is interpreted as the crystallization age, in agreement with the anatexis age obtained in the Quatro Cachoeiras paragneiss (c. 1530 Ma). The older age (c. 1800 Ma) suggests inherited zircon from calc-alkaline rocks generated in the early stages of the Juruena Arc (1.82-1.74 Ga), deposited previously in the Quatro Cachoeiras basin.

5. Ar-Ar step heating results

5.1. Analytical procedures

The four selected samples (RB-16A, UP-25C, UP-27A and FS-66; Table 1) were first examined under a petrological microscope to assess the level of alteration of the phase to be analyzed (0.5 to 1.0 mm diameter amphibole and muscovite). These single amphibole and muscovite grains were $^{40}Ar/^{39}Ar$ step-heated with a Synrad® CO^2 continuous laser and isotopic analyses of the five evolved argon isotopes were performed on a MAP215® noble gas mass spectrometer at Geosciences Rennes. All isotopic measurements are corrected for mass discrimination and atmospheric argon contamination. following Lee et al. (2006) and Mark et al. (2011), as well as K, Ca and Cl isotopic interferences. The decay constants used are from Renne et al. (2011). Samples and standards (Amphibole Hb3gr; age: 1081.0 ± 0.11% Ma; Renne et al. 2011) were co-irradiated with Cd-shielding for 298 hours at the McMaster reactor (Hamilton. Canada. location 8E) with a J/h of 5.86 x 10^{-6} x h^{-1}. Further analytical details are outlined by Ruffet et al. (1991, 1995). Apparent age errors are plotted at the 1σ level and do not include the errors on the $^{40}Ar^*/^{39}ArK$ ratio and age of the monitor and decay constant. Plateau ages were calculated if 70% or more of the 39ArK was released in at least three or more contiguous steps. the apparent ages of which agreeing to within 1σ of the integrated age of the plateau segment. The errors on the $^{40}Ar^*/^{39}ArK$ ratio and age of the monitor and decay constant are included in the final calculation of the error margins on the pseudo-plateau age or on apparent ages individually cited. The $^{40}Ar/^{39}Ar$ age spectra are shown in Figure 6.

TABLE 3. Field and textural characteristics of the Juruena rocks in RGTB, submitted to geochronological analysis, represented by Granite-gneiss Domain: (A) augen gneiss, (B) isotropic granites, (C,D) phyllonites, (E) foliated granitoids; and Supracrustal Domain: (F) S-type leucogranites, (G) stromatic metatexite leucosome rich (migmatite paragnaisses) and (H) amphibolites

					isotopic ratios (Pb^{204} corrected)								Ages (1 sigma)				
Spot	U ppm	Th ppm	Th/U	^{206}Pb ppm	$^{207}Pb/^{206}Pb$		$^{207}Pb/^{235}U$		$^{206}Pb/^{238}U$		$^{208}Pb/^{232}Th$		$^{206}Pb/^{238}U$		$^{206}Pb/^{207}Pb$		Conc. %
RB-16A, Hornblende-biotite monzogranite (augen gneiss), Igarapé das Lontras Suite, zircon - U-Pb LA-ICP-MS																	
Z1	n.a.	n.a.	n.a.	n.a.	0.1150	n.a.	5.488	± 5.4	0.3463	± 3.9	n.a.	n.a.	1917	± 64	1879	± 67	102.05
Z3	96.97	n.a.	96.97	n.a.	0.1112	n.a.	4.919	± 5.8	0.3323	± 4.1	n.a.	n.a.	1694	± 53	1819	± 64	93.14
Z7	50.50	n.a.	50.50	n.a.	0.1106	n.a.	4.655	± 7.5	0.3122	± 5.3	n.a.	n.a.	1777	± 123	1810	± 145	98.18
Z16	45.88	n.a.	45.88	n.a.	0.1073	n.a.	4.552	± 6.2	0.3062	± 4.3	n.a.	n.a.	1850	± 66	1755	± 75	105.40
Z4	57.00	n.a.	57.00	n.a.	0.1081	n.a.	4.722	± 6.8	0.3171	± 4.8	n.a.	n.a.	1751	± 81	1768	± 97	99.06
Z5	50.48	n.a.	50.48	n.a.	0.1078	n.a.	4.670	± 5.3	0.3100	± 3.7	n.a.	n.a.	1722	± 66	1763	± 80	97.71
Z6	45.65	n.a.	45.65	n.a.	0.1080	n.a.	4.489	± 6.1	0.3054	± 4.3	n.a.	n.a.	1776	± 74	1766	± 88	100.55
Z9	92.08	n.a.	92.08	n.a.	0.1093	n.a.	4.679	± 5.3	0.3176	± 3.8	n.a.	n.a.	1741	± 57	1787	± 68	97.40
Z12	54.34	n.a.	54.34	n.a.	0.1066	n.a.	4.840	± 5.8	0.3254	± 4.1	n.a.	n.a.	1718	± 65	1742	± 79	98.65
Z13	83.00	n.a.	83.00	n.a.	0.1068	n.a.	4.865	± 5.8	0.3226	± 4.1	n.a.	n.a.	1778	± 58	1746	± 69	101.83
Z14	83.56	n.a.	83.56	n.a.	0.1079	n.a.	4.594	± 5.2	0.3097	± 3.7	n.a.	n.a.	1816	± 64	1764	± 74	102.97
Z15	72.11	n.a.	72.11	n.a.	0.1094	n.a.	4.720	± 5.7	0.3158	± 4.0	n.a.	n.a.	1802	± 64	1789	± 74	100.75
Z17	91.08	n.a.	91.08	n.a.	0.1076	n.a.	4.520	± 7.3	0.3031	± 5.1	n.a.	n.a.	1739	± 56	1759	± 67	98.90
Z19	70.25	n.a.	70.25	n.a.	0.1084	n.a.	4.609	± 5.8	0.3108	± 4.0	n.a.	n.a.	1769	± 62	1773	± 73	99.81
Z21	104.11	n.a.	104.11	n.a.	0.1082	n.a.	4.770	± 5.6	0.3229	± 3.9	n.a.	n.a.	1706	± 77	1769	± 95	96.48
Z22	62.42	n.a.	62.42	n.a.	0.1076	n.a.	4.695	± 5.6	0.3178	± 3.9	n.a.	n.a.	1744	± 61	1759	± 76	99.19
Z26	139.20	n.a.	139.20	n.a.	0.1071	n.a.	4.627	± 9.9	0.3124	± 7.0	n.a.	n.a.	1804	± 61	1751	± 74	103.00
Z27	77.84	n.a.	77.84	n.a.	0.1071	n.a.	4.552	± 6.0	0.3111	± 4.2	n.a.	n.a.	1779	± 60	1751	± 73	101.60
Z28	31.33	n.a.	31.33	n.a.	0.1074	n.a.	4.539	± 5.1	0.3102	± 3.6	n.a.	n.a.	1752	± 107	1756	± 129	99.78
Z20	68.57	n.a.	68.57	n.a.	0.1061	n.a.	4.479	± 7.1	0.3079	± 5.0	n.a.	n.a.	1746	± 65	1734	± 79	100.72
Z8	85.00	n.a.	85.00	n.a.	0.1061	n.a.	4.651	± 5.5	0.3186	± 3.8	n.a.	n.a.	1742	± 55	1734	± 67	100.44
Z18	61.52	n.a.	61.52	n.a.	0.1055	n.a.	4.645	± 5.3	0.3248	± 3.6	n.a.	n.a.	1730	± 76	1723	± 92	100.39
Z24	78.26	n.a.	78.26	n.a.	0.1059	n.a.	4.720	± 8.8	0.3265	± 6.2	n.a.	n.a.	1783	± 60	1730	± 73	103.06
Z23	53.54	n.a.	53.54	n.a.	0.1037	n.a.	4.919	± 5.8	0.3323	± 4.1	n.a.	n.a.	1813	± 57	1692	± 70	107.15
Z25	61.89	n.a.	61.89	n.a.	0.1048	n.a.	4.655	± 7.5	0.3122	± 5.3	n.a.	n.a.	1821	± 99	1712	± 116	106.42
LB-31A. Biotite monzogranite, Teodósia Suite, zircon (type-area) - U-Pb SHRIMP II																	
0824A.6-1	283	295	1.08	75.5	0.1070	± 1.5	4.5587	± 1.9	0.3090	± 1.2	0.0913	± 20.4	1731.2	± 22.1	1749	± 27	99.20
0824A.11-1	191	177	0.96	50.7	0.1076	± 0.7	4.5951	± 1.5	0.3099	± 1.2	0.0881	± 20.2	1744.1	± 22.7	1758	± 13	98.90
0824A.3-2	79	55	0.72	21.4	0.1076	± 1.0	4.6824	± 1.9	0.3157	± 1.6	0.0911	± 20.0	1769.2	± 26.6	1759	± 19	100.60
0824A.1-1	86	49	0.59	23.3	0.1068	± 1.4	4.6559	± 2.1	0.3161	± 1.5	0.0904	± 20.2	1772.2	± 25.4	1746	± 26	101.40
0824A.1-2	111	71	0.67	30.1	0.1069	± 0.9	4.6715	± 1.7	0.3168	± 1.4	0.0905	± 10.8	1776.3	± 24.2	1748	± 17	101.50
0824A.4-2	72	45	0.65	19.7	0.1071	± 1.1	4.6872	± 1.9	0.3173	± 1.6	0.0929	± 20.1	1774.9	± 26.7	1751	± 21	101.40
0824A.4-1	136	89	0.68	37.1	0.1065	± 0.9	4.6726	± 1.6	0.3182	± 1.4	0.0936	± 10.7	1778.7	± 23.3	1740	± 16	102.30
0824A.3-1	125	89	0.73	34.4	0.1062	± 0.8	4.6896	± 1.6	0.3204	± 1.4	0.0929	± 10.7	1791.2	± 24.2	1735	± 16	103.30
0824A.9-1	69	38	0.57	19.1	0.1076	± 1.2	4.7866	± 2.0	0.3226	± 1.6	0.0930	± 20.4	1802.9	± 27.2	1759	± 22	102.50
0824A.5-1	147	130	0.92	40.7	0.1059	± 0.9	4.7184	± 1.7	0.3232	± 1.4	0.0909	± 10.9	1811.2	± 25.9	1729	± 17	104.40
GH-03A. Mylonitic biotite granite, Teodósia Suite, zircon - U-Pb SHRIMP II																	
D1117.8-1	646	999	1.55	171.6	0.1082	± 0.3	4.5935	± 1.0	0.3092	± 1.0	0.0862	± 1.2	1736.9	± 15.0	1762	± 07	98.60
D1117.8-2	382	367	0.96	100.3	0.1070	± 0.4	4.5144	± 1.1	0.3059	± 1.0	0.0867	± 1.3	1720.3	± 15.6	1750	± 08	98.32
D1117.3-1	350	339	0.97	92.5	0.1068	± 0.4	4.5464	± 1.1	0.3080	± 1.0	0.0859	± 1.1	1730.9	± 15.8	1750	± 08	98.91
D1117.4-1	384	436	1.13	99.1	0.1061	± 0.5	4.4134	± 1.4	0.3003	± 1.3	0.0841	± 1.4	1692.8	± 18.8	1742	± 10	97.18
D1117.2-1	319	365	1.15	83.4	0.1076	± 0.5	4.5117	± 1.4	0.3046	± 1.2	0.0859	± 1.4	1714.1	± 19.3	1756	± 09	97.60
D1117.7-1	564	662	1.17	149.5	0.1065	± 0.4	4.5133	± 1.4	0.3085	± 1.3	0.0855	± 1.4	1733.5	± 19.3	1733	± 10	100.01
D1117.6-1	432	476	1.10	113.3	0.1077	± 0.7	4.5298	± 1.5	0.3051	± 1.3	0.0847	± 1.4	1716.5	± 20.0	1761	± 13	97.50
GH-03A. Mylonitic biotite granite, Teodósia Suite, titanite - U-Pb SHRIMP II																	
A1117.1-1	159	145	0.91	1.18	0.1185	± 0.7	4.6871	± 1.9	0.3143	0.9	0.3091	1.2	1761.6	± 13.8	1769	± 30	99.59
A1117.1-2	148	132	0.89	1.58	0.1194	± 0.7	4.5760	± 2.1	0.3142	0.9	0.3392	1.2	1761.4	± 13.9	1725	± 34	102.09
A1117.1-3	133	112	0.84	1.57	0.1202	± 0.7	4.5385	± 2.3	0.3088	1.0	0.4284	1.3	1734.8	± 14.7	1742	± 38	99.59

TABLE 3 (continuation)

Spot	U ppm	Th ppm	Th/U	^{206}Pb ppm	isotopic ratios (Pb^{204} corrected) $^{207}Pb/^{206}Pb$		$^{207}Pb/^{235}U$		$^{206}Pb/^{238}U$		$^{208}Pb/^{232}Th$		Ages (1 sigma) $^{206}Pb/^{238}U$		$^{206}Pb/^{207}Pb$		Conc. %
AA-22B. Migmatitic paragneiss, Quatro Cachoeiras Complex, zircon - U-Pb SHRIMP II																	
E1117.3-2	79	63	0.82	20.8	0.1083	± 1.2	4.5653	± 1.9	0.3063	± 1.5	0.0878	± 2.0	1722.5	± 22.4	1802	± 21	95.59
E1117.5-2	306	212	0.71	81.8	0.1077	± 0.6	4.6157	± 1.3	0.3108	± 1.1	0.0867	± 1.3	1744.6	± 16.8	1761	± 11	99.07
E1117.4-1	92	65	0.73	24.4	0.1078	± 1.3	4.5655	± 1.9	0.3072	± 1.4	0.0836	± 2.3	1726.7	± 21.8	1763	± 24	97.97
E1117.3-3	317	247	0.81	85.3	0.1076	± 0.5	4.6170	± 1.2	0.3108	± 1.1	0.0855	± 1.4	1744.4	± 16.7	1739	± 12	100.29
E1117.1-1	899	392	0.45	203.1	0.0962	± 0.4	3.4833	± 1.1	0.2628	± 1.0	0.0723	± 1.3	1504.0	± 13.3	1556	± 09	96.65
E1117.6-1	50	30	0.62	11.3	0.0951	± 2.1	3.4326	± 2.7	0.2618	± 1.7	0.0746	± 3.2	1499.1	± 22.4	1530	± 40	97.96
E1117.2-1	200	133	0.69	46.2	0.0950	± 0.8	3.5214	± 1.4	0.2689	± 1.2	0.0776	± 1.5	1535.2	± 16.3	1528	± 15	100.50
E1117.5-1	631	388	0.64	143.7	0.0949	± 0.5	3.4656	± 1.1	0.2649	± 1.0	0.0756	± 1.2	1514.8	± 13.7	1526	± 09	99.27
E1117.3-1	42	23	0.56	9.5	0.0948	± 1.5	3.4035	± 2.2	0.2596	± 1.7	0.0715	± 4.2	1487.9	± 22.2	1491	± 30	99.79
AA-32. Amphibolite, Quatro Cachoeiras Complex, zircon - U-Pb SHRIMP II																	
1213D.5-1	170	96	0.56	44.1	0.1115	± 0.8	4.5079	± 1.6	0.3006	± 1.1	0.0877	± 1.5	1699.7	± 17.0	1779	± 22	95.22
1213D.5-2	215	147	0.69	57.0	0.1081	± 0.5	4.6100	± 1.1	0.3092	± 0.9	0.0876	± 1.2	1740.5	± 15.4	1768	± 10	98.21
1213D.5-3	423	2	0.01	110.5	0.1077	± 0.4	4.4990	± 0.9	0.3038	± 0.8	0.0984	± 4.5	1710.4	± 12.8	1756	± 07	97.37
1213D.1-1	631	4	0.01	167.2	0.1075	± 0.3	4.5633	± 0.9	0.3083	± 0.9	0.0897	± 3.7	1732.5	± 13.4	1755	± 06	98.71
1213D.2-1	112	40	0.35	29.9	0.1080	± 0.7	4.5926	± 1.3	0.3102	± 1.1	0.0889	± 1.6	1744.1	± 16.9	1755	± 14	99.22
1213D.3-1	673	5	0.01	177.0	0.1078	± 0.3	4.5488	± 1.0	0.3062	± 0.9	0.0894	± 3.4	1721.8	± 13.7	1762	± 06	97.72
1213D.10-1	188	118	0.63	49.8	0.1131	± 0.6	4.5716	± 1.4	0.3066	± 1.0	0.0938	± 1.3	1727.6	± 16.4	1768	± 19	97.52
1213D.10-2	503	318	0.63	131.2	0.1098	± 0.7	4.5145	± 1.2	0.3026	± 0.9	0.0901	± 1.4	1704.4	± 14.2	1769	± 14	96.33
1213D.4-1	138	67	0.49	37.2	0.1079	± 0.7	4.6355	± 1.3	0.3137	± 1.0	0.0878	± 1.5	1764.5	± 16.9	1752	± 15	95.22
GH-12A. Two mica granodiorite, Itamarati Suite, zircon - U-Pb SHRIMP II																	
1109e.1-1	104	59	0.57	29.1	0.1101	± 0.9	4.9482	± 1.5	0.3260	± 1.2	0.0928	± 1.8	1818.8	± 18.8	1801	± 17	100.99
1109e.4-1-4	377	428	1.13	104.8	0.1116	± 0.5	4.9794	± 1.1	0.3236	± 0.9	0.0903	± 1.1	1807.4	± 14.6	1826	± 09	99.00
1109e.5-1	229	135	0.59	64.2	0.1098	± 0.7	4.9306	± 1.2	0.3256	± 1.0	0.0922	± 1.4	1817.0	± 15.3	1797	± 12	101.14
1109e.1-2	299	236	0.79	80.8	0.1101	± 0.5	4.7767	± 1.1	0.3147	± 0.9	0.0913	± 1.1	1763.7	± 14.1	1801	± 10	97.93
1109e.3-1-4	171	97	0.57	46.1	0.1106	± 0.9	4.7820	± 1.5	0.3136	± 1.1	0.0888	± 1.7	1758.4	± 17.3	1809	± 17	97.19
1109e.5-2-5	81	67	0.83	21.8	0.1109	± 1.8	4.7620	± 2.4	0.3115	± 1.6	0.0849	± 2.6	1747.8	± 24.8	1814	± 32	96.35
1109e.9-1	448	270	0.60	121.8	0.1097	± 0.5	4.7921	± 1.0	0.3169	± 0.9	0.0918	± 1.1	1774.3	± 13.4	1794	± 08	98.89
1109e.6-1	280	188	0.67	77.0	0.1098	± 0.7	4.8425	± 1.2	0.3199	± 1.0	0.0931	± 1.3	1789.3	± 15.3	1796	± 12	99.63
1109e.7-1	343	146	0.43	80.0	0.0946	± 0.6	3.5364	± 1.1	0.2712	± 0.9	0.0776	± 1.3	1546.9	± 12.4	1520	± 12	101.80

Notes: Isotopic ratios errors in %; All Pb in ratios are radiogenic component, All corrected for ^{204}Pb. disc. = discordance, as 100 - 100{t[$^{206}Pb/^{238}U$]/t[$^{207}Pb/^{206}Pb$]} ; 4f206 = (common ^{206}Pb) / (total measured ^{206}Pb) based on measured ^{204}Pb. Uncertainties are 1σ; n.a.=not available.

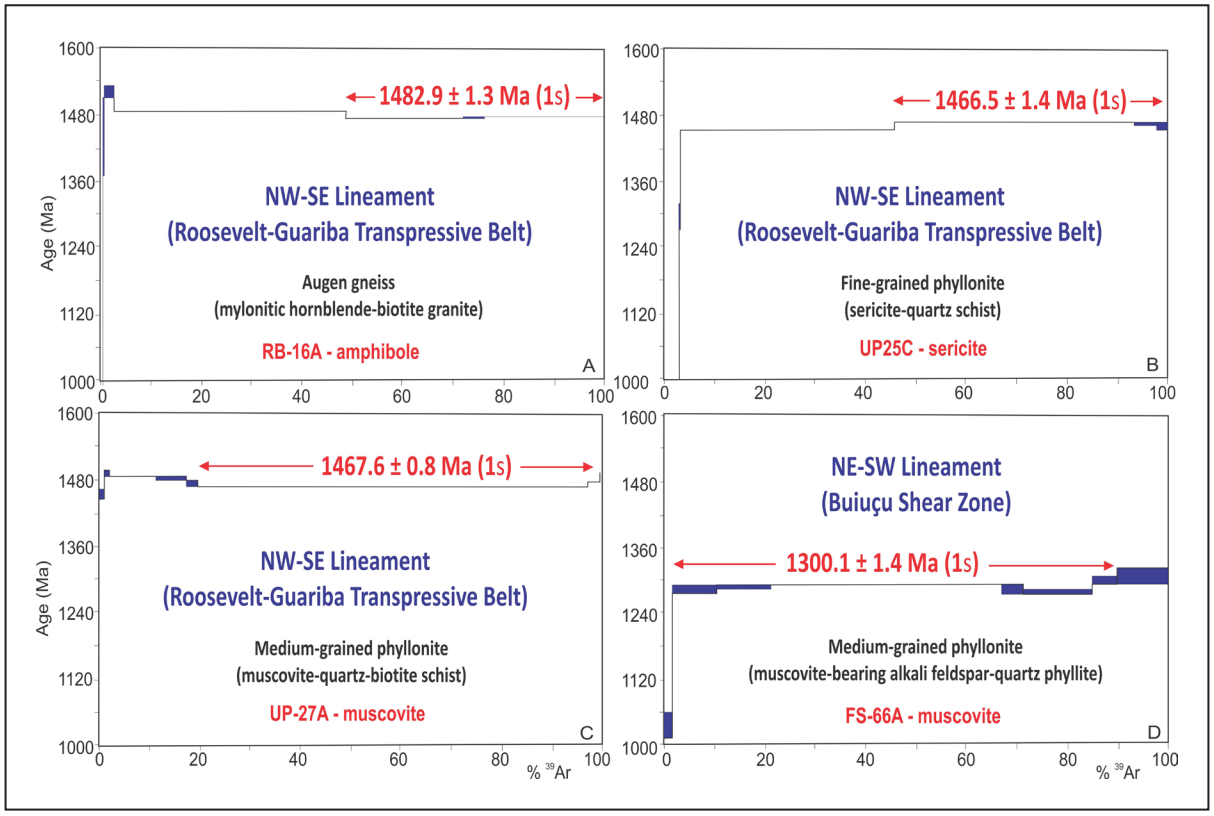

FIGURE 6. $^{40}Ar/^{39}Ar$ stepwise heating results (plateau ages) obtained in the analyzed samples: A. amphibole in augen gneiss (RB-16A; mylonitic hornblende-biotite granite); B. sericite in fine-grained phyllonite (UP-25C; sericite-quartz schist); C. muscovite in medium-grained phyllonite (UP-27A; muscovite-quartz-biotite schist); D. muscovite in medium-grained phyllonite (FS-66A; muscovite-bearing alkali feldspar-quartz phyllonite). All protoliths are sheared felsic subvolcanic/local plutonic rocks of the Igarapé das Lontras Suite and subvolcanic rocks of the Colíder Group (see tables 1 and 2).

5.2 Augen gneiss, meta(sub)volcanic rocks, metamicrogranites and phyllonites (Colíder Group and Igarapé das Lontras Suite): amphibole, muscovite and sericite Ar-Ar ages

The high-temperature mylonitic granite (hornblende-biotite augen gneiss) represented by the RB-16A sample (Roosevelt River) yielded a plateau age of 1482 ± 1.3 Ma based on amphibole grains (Figures 3A and 6A). This age points to a Calymmian tectonothermal event at ~580°C taking in account the estimate blocking temperature for amphiboles in the Ar-Ar isotopic system (e.g. Kamber et al. 1995).

Muscovite and sericite from two phyllonites of the Roosevelt River (Figure 2) were also analyzed. These rocks are represented by muscovite-quartz-biotite-schist and sericite-quartz schist, which protoliths correspond to fine do medium-grained sheared granites (Igarapé das Lontras Suite). Both phyllonites are also associated to regional NW-trending shear zones of the Roosevelt-Guariba Deformation Belt (RGDB). The UP-25C (muscovite) and UP-27A (sericite) samples yielded *plateau ages* respectively of 1466.5 ± 1.4 Ma (1σ) and 1467.6 ± 0.8 Ma (1σ) (Figures 3C,D and 6B,C), corresponding to a maximum cooling age for the tectonothermal event of 420°-510°C, according to the estimate blocking temperature for the white micas in the Ar-Ar isotopic system (Kirschner et al. 1996a, b).

A third phyllonite sample, located in the Buiuçu River (Figure 2), is associated with NE-trending regional shear zones (Buiuçu Shear Zone - BSZ), whose felsic hypabyssal to volcanic rocks protoliths are sheared (Colíder Group), transformed into muscovite-bearing alkali feldspar-quartz phyllonites. This sample (FS-66A; muscovite) yielded a plateau age of 1300.1 ± 1.4 Ma (1σ) (Figure 6D), showing a 160 Ma younger event with temperatures ranging from 510°C to 420°C (Kirschner et al. 1996a, b).

6. Discussions

6.1 Crustal evolution and events chronology

A model based on accretionary origin is the most frequently invoked for the Juruena Terrain. According to Scandolara et al. (2016), the Juruena Accretionary Belt is composed of the Jamari and Juruena arc systems generated in an Andean-type continental margin during Sthaterian-Orosirian times (e.g. Duarte et al. 2012; Ribeiro and Duarte 2010; Santos et al., 2000; Scandolara et al. 2013, 2014; Souza et al. 2005; Tassinari and Macambira 1999) with magmatic flare up in the 1780-1760 Ma interval (Figures 7 and 8). The geochronological data indicate a continuous calc-alkaline magma generation from 1.85 to 1.73 Ga in the Juruena Accretionary Belt (Table 1; e.g. Silva and Abram 2008; Ribeiro and Duarte 2010; Duarte et al. 2012; Scandolara et al. 2014) showing several regional denominations: Juruena (1850-1820 Ma), Paranaíta (1820-1790 Ma), Vitória and Vespor suites, São Pedro and São Romão granites (1785-1765 Ma), Teodósia Suite and orthoderived types of Jamari Complex (1760-1730 Ma).

In the Juruena Terrain the intensity of regional EW deformation (D1 event) decreases from southwest to northeast (Oliveira and Almeida 2021) and is cross-cut by the NW-SE trending Roosevelt-Guariba Transpressive Belt (D2 event). The Roosevelt-Guariba Transpressive Belt (RGTB) reworked these earlier structures (D1) during Calymmian times (Figure 7) under high-T and medium-P conditions (Figure 9, D2 event; Oliveira and Almeida 2021). Also during Calymmian were emplaced bimodal magmatism (Serra da Providência and Matá-Matá suites) and crustal-derived two mica granites (Itamaraty Suite). The development of RGTB and magma generation (bimodal and crustal-derived, post-orogenic within-plate magmatism) are attributed to an intracontinental evolution (Figure 7; Oliveira and Almeida 2021), related to distal pericontinental deformation and metamorphism during the Rondoniano-San Inácio/Cachoeirinha orogeny (Figure 9).

The 1480-1460 Ma Ar-Ar ages are related to the NW-trending shear zones generation, responsible for the installation of the Roosevelt-Guariba Deformational Belt (RGDB) according to Oliveira (2016) and Oliveira and Almeida (2021). On the other hand, the 1300 Ma Ar-Ar age, related to the NE-trending shear zones (Buiuçu Fault), may be interpreted as a hinterland reflex of the Sunsás Orogeny (Santos et al. 2008) or Rondonian-San Inácio Orogeny (Bettencourt et al. 2010), at the northeasternmost point of Rondônia-Juruena Province. Only in the westernmost area (Jamari Domain; Scandolara 2006) are observed magmatic rocks with 1315-1310 Ma (São Lourenço-Caripunas Suite), generated in the late stages of this orogeny (Bettencourt et al. 1999).

Finally, the Beneficent and Palmeiral Basins (Figures 7 and 8) played an important role in the cratonization of the Juruena Terrain, developed between 1.40 Ga and 1.00 Ga (Oliveira and Almeida, 2021; Reis et al. 2013, 2017). Younger structures are related to the crustal reactivations (Oliveira and Almeida 2021), controlling the gold mineralizations in the region (D3) or as NW-SE late normal faults (D4) associated mainly with the Paleozoic basins (Toczeck et al. 2019).

According to Oliveira (2016) and Oliveira and Almeida (2021), the geotectonic framework of Juruena Terrain in the southeastern Amazonas is compatible with an evolution as a foreland basin developed over the Tapajós-Parima basement during the Juruena Orogeny (1.82-1.74 Ga). Thick and wide supracrustal successions and older weakness zones are also associated with the development of this foreland basin, which in turn is preserved from regional metamorphism and deformation (D1, E-W structures) of the late Statherian (1.67-1.63 Ga).

However, this orogenic model is not consensus, and since Montavão et al. (1984) and Neder et al. (2000) a within plate extensional model is proposed, related to late- and post-tectonic stages of Tapajós-Parima Orogeny (2.00-1.88 Ga; Pinho et al. 2003). For example, the Juruena Terrain was redefined as the Western Amazonia Igneous Belt (Rizzotto et al. 2019a, b), whose within plate extensional evolution (Tapajós-Parima Rift) is related to magmatig underplating. The "Hot Orogens" (Collins 2002) along with many high-grade metamorphic terrains that typify continental crust, most formed in accretionary orogens during tectonic switching, when prolonged lithospheric extension was interrupted by intermittent, transient contraction. Based on modern and ancient examples, tectonic switching occurs when slab retreat induces upper plate extension, causing arc splitting, formation of microcontinent slivers, and back-arc basins; then intermittent arrival of buoyant oceanic plateaus induces transient flat subduction (or slab flip model is also proposed, describing extensional and compressional alternating events associated to plate margin as a response to dip-angle subduction variations (Alves et al. 2013; Diener et al. 2019; Duarte et al. 2019; Trindade Netto et al. 2020).

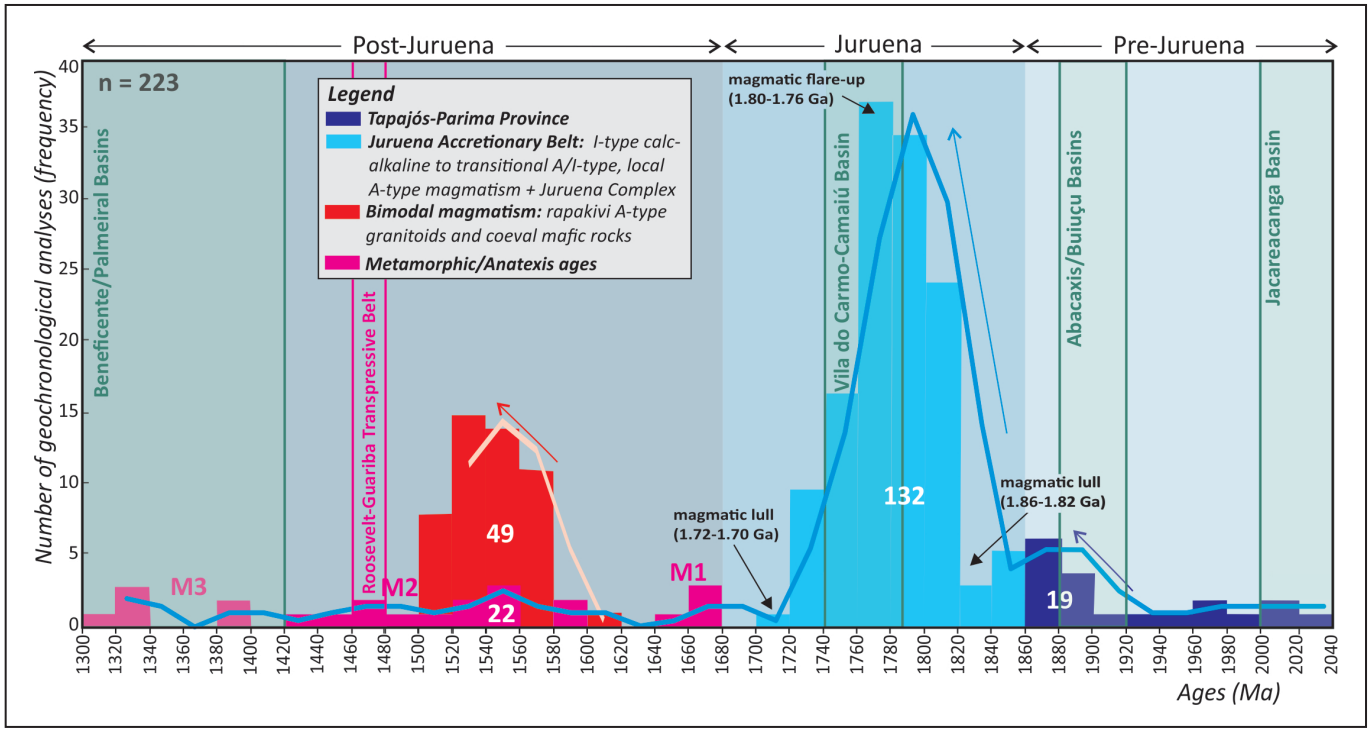

FIGURE 7. Simplified sketch of the tectonic evolution of the Juruena Terrain in the SE Amazonas, showing main domains and magmatic and (volcano)sedimentary events (Oliveira and Almeida 2021).

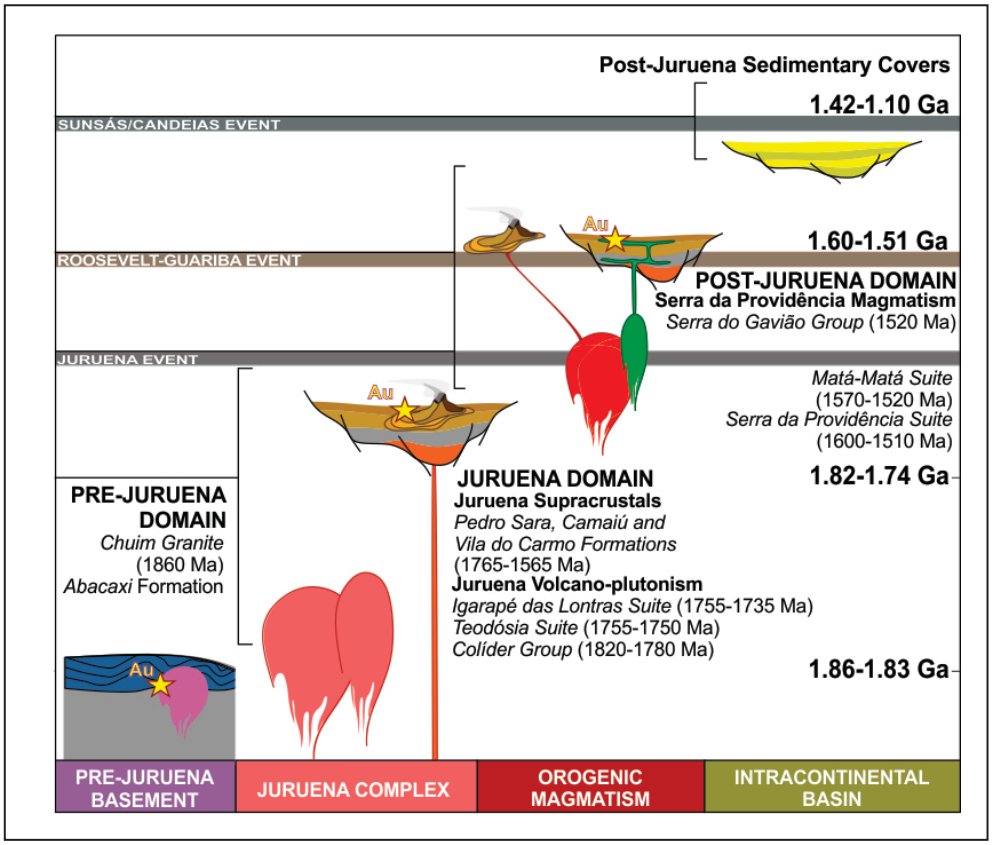

FIGURE 8. Histogram ages showing the temporal distribution of Paleoproterozoic to Mesoproterozoic events of the Juruena Terrain in the SE Amazonas, North Mato Grosso and NE Rondônia. For references, methods and numbers see table 3. For other data see references in the text.

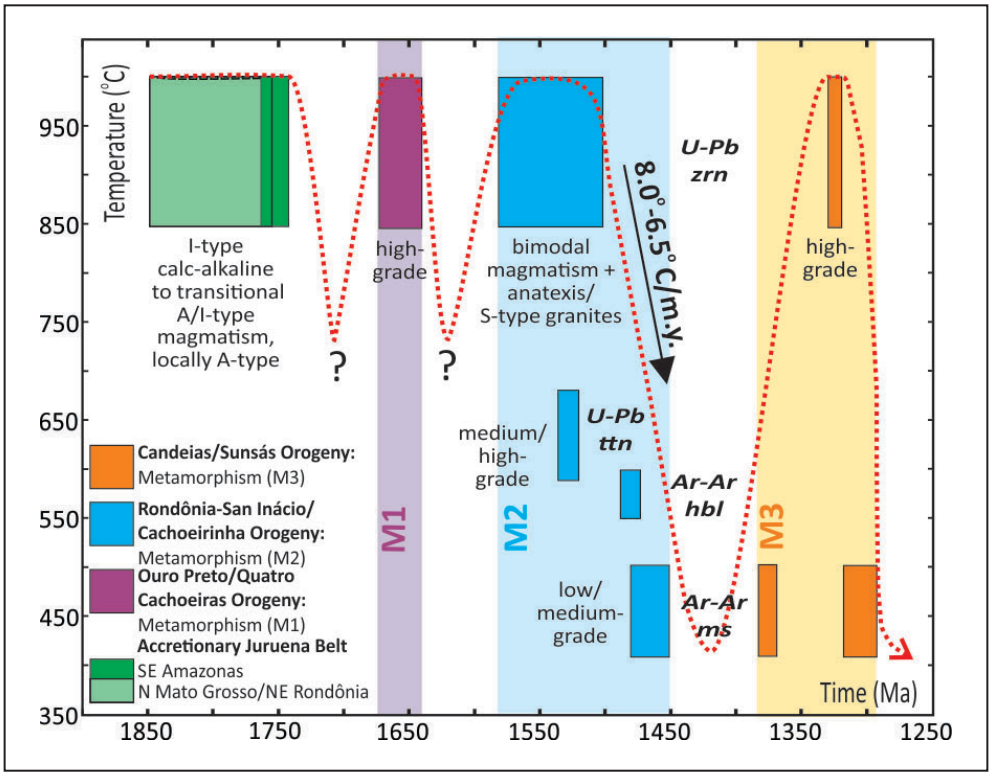

FIGURE 9. Estimative Time vs temperature path of the Juruena Terrain based on geochronological data (see also Table 3). The closure temperatures (minerals/methods) are in agreement with Grove and Harrison (1996), Kamber et al. (1995) and Purdy and Jäger (1976).

6.2 The Juruena Terrain and the evolution of the Columbia Supercontinent

Considering the Supercontinent cycles and available paleomagnetic data, the Juruena Accretionary Belt (1.85-1.73 Ga) probably was involved in the final amalgamation stages of the Paleoproterozoic Columbia supercontinent (e.g. Bispo-Santos et al. 2008), showing apparent long-lived connections with Laurentia (Yavapai Province) and Baltica (Transscandinavian Belt). Some paleomagnetic data (e.g. Bispo-Santos et al. 2008, 2014; D´Agrella-Filho et al. 2016) favors the idea that the Amazon Craton joined the Columbia supercontinent at ~1790 Ma ago, in a similar scenario of the South America and Baltica configuration (SAMBA), according to Johansson (2009) and Bispo-Santos et al. (2008, 2014). Based on these paleomagnetic data, Baltica, Laurentia and Amazonia remained quasi-stationary for a long time (from 1780 Ma to 1540 Ma), generating a large continental mass (core of Columbia) in Paleo-Mesoproterozoic times (Figure 10).

Over this time, on the western side of Columbia, subduction-related accretionary belts were developed (e.g. Pesonen et al. 2012; Salminen et al. 2016, Almeida et al. 2022), similar in age of the Juruena Accretionary Belt. The participation of the Juruena Terrain in the SAMBA (South AMerica-BAltica) model, forming the core of the Columbia supercontinent, is constrained by the 1.79 Ga Colíder pole (Bispo-Santos et al. 2008) and supported by geochronological data correlations (Johansson 2009), with the Amazonian, Laurentia and Baltica evolution between ~1.80 Ga and ~1.50 Ga showing several geological and tectonic similarities. In the western margin of Columbia, the SW Amazon Craton is characterized by a long-lived arc system, showing medium K calc-alkaline to shoshonitic magmatism (1850-1730 Ma), correlated to the same accretionary systems in Yavapai Province (Laurentia) and Transscandinavian Igneous Belt (Baltica).

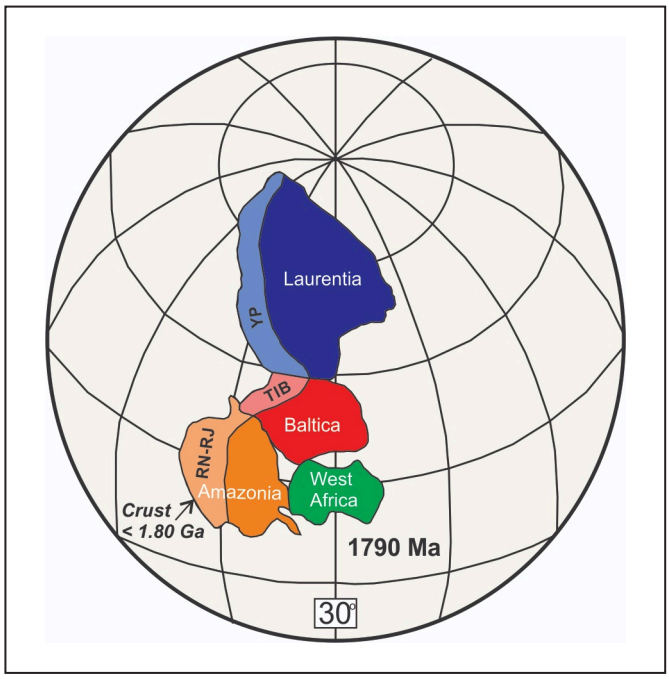

FIGURE 10. Paleogeographic global reconstruction of Laurentia-Baltica-Amazonia-West Africa at ~1790 Ma forming the core of Columbia Supercontinent (simplified after Bispo-Santos et al. 2014, 2020). The boundaries of Rio Negro and Rondônia-Juruena Provinces (RN-RJ), Transscandinavian Igneous Belt (TIB) and Yavapai Province (YP) are approximated.

According to Whitmeyer and Karlstrom (2007), the Yavapai Province is defined as a wide zone with upper a 2000 km of predominantly juvenile arc with 1.80 to 1.70 Ga. Furthermore, collisions and an orogenic peak (Yavapai Orogeny) at 1.71–1.68 Ga results in a progressive amalgamation of Yavapai crust to Laurentia Craton. In the Grenville Province (e.g. Gower and Krogh 2002) rocks older than 1710 Ma (pre-Labradorian) were generated also in a continental-margin basin, subsequently destroyed during the accretion of a magmatic arc with a short-lived subduction zone.

Western Baltica in the late Paleoproterozoic shows convergent-margin tectonics (e.g. Åhäll et al. 2002; Johansson 2021) resulting in the Transscandinavian Igneous Belt (TIB) with 1400 km in extension and westward younging growth (Gothian Zone). This westward younging of the magmatism in the TIB (cf. Åhäll et al. 2002; Wahlgren and Stephens 2020; Stephens and Bergman 2020; Johansson 2021) is demonstrated by TIB-0 (1.86-1.83 Ga), TIB-1 (1.81–1.77, dominant) Ga, TIB-2 (1.71-1.69 Ga) and Gothian (1.66-1.50 Ga) magmatism. In the Juruena Accretionary Belt (~ 1000 km), Juruena magmatism (1.80-1.75 Ga) is clearly correlated to TIB-1, and the Jamari magmatism (1.76-1.73 Ga) shows intermediate ages among TIB-1 and TIB-2. Early magmatism in the Juruena Complex (1.85-1.81 Ga), correlated to TIB-0, is subordinated, located near the boundaries of the Tapajós crust (Tapajós-Parima Province, 2.05-1.86 Ga), this last one correlated with the Svecofennian crust (2.10-1.87 Ga). The Juruena Acrettionary Belt in this sense shows also the same westward younging growth, similarly the NW Amazon Craton (e.g. Almeida et al. 2022) and the Transscandinavian Igneous Belt (e.g. Högdahl et al. 2004).

Younger magmatic events with Calymmian age are present in the Juruena Accretionary Belt, represented by two main types: a) abundant bimodal association with A-type rapakivi granite dominant (Serra da Providência Suite, 1.57-1.50 Ga) and b) local S-type granites (Itamaraty Suite, 1.55-1.52 Ga) in association with high-grade paragneisses (Quatro Cachoeira Complex), suggesting minor crustal reworking and anatexis. This 1.55-1.52 Ga high-grade event is probably related to the early stages of the Rondonian-San Inácio/Cachoeirinha Orogeny (1.54-1.46 Ga), most common in the western margin of the SW Amazon Craton, producing distal orogenic processes responsible for the broad Calymmian granitic magmatism observed in the Juruena Terrain (Oliveira and Almeida 2021). In the Grenville Province, the Pinwarian Orogeny is also characterized by abundant Calymmian granitoids (1526-1466 Ma; igneous zircon, Tucker and Gower 1994, Heaman et al. 2004) and locally migmatized paragneiss (1640 ± 7 Ma, detrital zircon, Tucker and Gower 1994). The K-granites and AMCG associations (inboard magmatic arc) are dominant, but no crustal-derived granites are described (i.e. S-type granites).

The Juruena Accretionary Belt was strongly reworked by other tectonothermal events (Figure 9), such as Ouro Preto/Quatro Cachoeiras (1.67-1.63 Ga) and Candeias/Sunsás orogenies (1.37-1.30 Ga). The older tectonothermal event (Ouro Preto/Quatro Cachoeiras Orogeny), not recorded in the study area (only in northern Mato Grosso), is probably associated with the final Columbia Supercontinent assembly and responsible by the E-W Juruena Belt framework. Effects of the final stages of the Candeias/Sunsás Orogeny were

observed in the NE-trending shear zones (Buiuçu Shear Zone), presumably related to Columbia Supercontinent break-up (e.g. Zhao et al. 2004).

7. Conclusions

The proposed model for the Juruena Terrain in the southeastern of Amazonas (Oliveira and Almeida 2021) is reinforced by the new and previous geochronological data. The Sthaterian arc-related rocks (ortho and paraderived) are deformed by several events under different temperatures during Calymmian and Ectasian times, which shaped the architecture of the Roosevelt-Guariba Transpressive Belt (NW-trending):

1. Quatro Cachoeiras Complex is interpreted as an arc-related basin (foreland) developed in the extensional setting in the final stages of the Juruena Accretionary Belt evolution, showing only one 1.75 Ga detrital zircon population (arc basement provenance). In the type area (northeast Rondônia), these migmatitic paragneisses show variable provenances, suggesting basement rock contributions from the Tapajós-Parima Province (1.92 Ga and 1.87-1.84 Ga) and Ouro Preto Orogeny rocks (1.67-1.63 Ma; Santos et al. 2003).

2. Widespread Calymmian high-T tectonothermal event (1545-1530 Ma; 600°-900°C Figure 9) affected the Jamari (NE Rondônia) and Juruena (southeast Amazonas) Terrains at a crustal-scale, producing migmatization (Quatro Cachoeiras Complex) and local crustal-derived magmatism (two-mica granites). The differences are related to the inherited ages of the two-mica granites, reflecting the particularities (sources and metamorphism) of the geological context of each Terrain. In the final stages, this Calymmian tectonothermal event shows lower temperatures (1483-1466 Ma, 580°-420°C; Figure 9), showing agreement with U-Pb detrital/magmatic zircon ages related to the Rondonian-San Inácio or Cachoeirinha orogenies (e.g. Geraldes et al. 2001; Payolla et al. 2003a, b; Reis et al. 2013).

3. Based on Ar-Ar (amphibole, muscovite, sericite) and U-Pb (zircon, titanite) geochronological data, the estimated cooling rates range from 8.0°C/m.y. to 6.5°C/m.y. (1520-1470 Ma), suggesting high to moderate exhumation rates (4-5 km) and fast uplift of Juruena Terrain in Sthaterian-Calymmian times during Roosevelt-Guariba Transpressive Belt intracratonic evolution (Figure 9). These high cooling rates, and probably sharp exhumation, allowed intense denudation of the deepest crust formed by orthogneisses and metagranitoids, with only a restricted nucleus of preserved paraderived migmatites and rare metavolcanic rocks. Thus, the 1.48-1.47 Ga interval age is probably representative of the NW-trending of the RGTB in the Northern Juruena Terrain;

4. The later tectonothermal event (1300 Ma), recorded in the Buiuçu Shear Zone (NE-trending). shows temperatures of 510°-420°C (Ar-Ar, muscovite). This event is interpreted as the reactivation of older fault zones (infracrustal older basement according to Oliveira, 2016), probably related to final stages of the Candeias/Sunsás Orogeny (1.37-1.32 Ga).

The correlation of these tectonothermal events and magmatic associations with Baltica and Laurentia point to an important role of the Juruena Terrain (in the Columbia/Nuna Supercontinent building. The Juruena Accretionary Belt (1200 km, EW- to NW-trending), together with the Trans-Scandinavian Igneous Belt (1400 km, NS-trending) and Yavapai Province (2000 km, NE-trending Supercontinent), formed in the Paleoproterozoic the core of the Columbia Supercontinent (e.g. Bispo-Santos et al. 2008, 2014), joining Amazon, Laurentia and Baltica continents (Scandolara et al. 2016). Subsequent tectonothermal events, related to the several orogenies, reworked strongly this accretionary belt at different times (1.67-1.63 Ga; 1.54-1.46 Ga; 1.37-1.30 Ga), defining the tectonic-structural framework currently observed.

Acknowledgements

The authors wish to express their gratitude to C.A. Salazar (UFAM) and A. Ruiz (UFMT) for profitable discussions and suggestions. Many thanks to all valuable colleagues on the many unforgettable journeys in Amazon lands, mainly N.J. Reis, R.B.C. Bahia, U.A.P. Costa, L. Betiollo, M. Neves and F. Splendor (in memoriam) and the field workers of the Geological Survey of Brazil-CPRM (GSB-CPRM). Thanks to the GSB-CPRM for financial support of analyses and field surveys (Sumaúma-Mutum-Roosevelt Project), and to Universidade Federal do Amazonas, Université de Rennes and University of Western Australia for laboratory support. Finally, many thanks to Denis Thiéblemont and one anonymous reviewer, and to Section Editor Henri Masquelin who provided extremely constructive comments that greatly assisted the revision and improved the work.

Authorship credits

Author	A	B	C	D	E	F
MEA						
ACSO						
JOSS						
JBR						
GR						

A - Study design/Conceptualization **B** - Investigation/Data acquisition
C - Data Interpretation/ Validation **D** - Writing
E - Review/Editing **F** - Supervision/Project administration

References

Acevedo Serrato A.A. 2014. Geocronologia e evolução do sistema hidrotermal do depósito aurífero de Juruena, província aurífera de Alta Floresta (MT), Brasil. MSc Dissertation, Instituto de Geociências, Universidade de Campinas. Available on line at: https://hdl.handle.net/20.500.12733/1622415 / (accessed on 10 November 2022)

Åhäll K.-I., Connelly J.N., Brewer, T.S. 2002. Transitioning from Svecofennian to Transscandinavian Igneous Belt (TIB) magmatism in SE Sweden: implications from the 1.82 Eksjö tonalite. GFF, 124, 217–224. https://doi.org/10.1080/11035890201244217

Almeida M.E, Nascimento R.S.C., Mendes T.A.A., Santos J.O.S., Macambira M.J.B., Vasconcelos P., Pinheiro S.S. 2022. An outline of Paleoproterozoic-Mesoproterozoic crustal evolution of the NW Amazon Craton and and implications for the Columbia Supercontinent. International Geology Review, 64, 1-34. https://doi.org/10.1080/00206814.2021.2025158

Almeida M.E., Costa U.A.P., Oliveira A.C.S. (org.). 2016. Geologia e recursos minerais da folha Sumaúma - SB.20-X-D, estado do Amazonas. Manaus, CPRM. 237 p. Escala 1:250.000. Available on line at: https://rigeo.cprm.gov.br/handle/doc/18292 / (accessed on 10 November 2022)

Almeida M.E.; Betiollo L.M., Splendor F., Costa. U.A.P., Bahia R.B.C., Brilhante J., Santos J.O.S. 2009. Aspectos geológicos, geoquímicos e geocronologia do zircão da Suíte São Romão no sudeste do Amazonas. In: Simpósio de Geologia da Amazônia, Manaus, AM.,

11, 115. Available on line at: https://sbg-no.org.br/arquivos/BASES/Anais%2011%20Simp%20Geol%20Amaz%20Agosto-2005-Manaus.pdf / (accessed on 10 November 2022)

Alves C.L., Rizzotto G.J., Rios F.S., de Barros M.A., S. 2020. The Orosirian Cuiú-Cuiú magmatic arc in Peixoto de Azevedo domain, Southern of Amazonian craton. Journal of South American Earth Sciences, 102, 102648. https://doi.org/10.1016/j.jsames.2020.102648

Alves C.L., Sabóia A.M., Martins E.G., Stropper J.L. (org.). 2010. Projeto Noroeste Nordeste de Mato Grosso: folhas São José do Xingu SC.22-Y-A e Rio Comandante Fontoura SC.22-Y-B. Goiânia: CPRM. Programa Geologia do Brasil (PGB). Levantamentos Geológicos Básicos. Available on line at: https://rigeo.cprm.gov.br/handle/doc/11359 / (accessed on 10 November 2022)

Alves C.L., Sabóia A.M., Scandolara J.E., Ribeiro P.S.E., Martins E.G. 2013. Magmatismo tipo A2 Colíder-Pium no SE do Cráton Amazônico, província Rondônia-Juruena – MT: litoquímica e geocronologia. In: Wankler F.L, Holanda E.C, Vasquez M.L. (org.). Contribuições à geologia da Amazônia, 8, 27–46. Available on line at: https://sbg-no.org.br/arquivos/BASES/CGA%208.pdf / (accessed on 10 November 2022)

Amaral G. 1974. Geologia pré-cambriana da região amazônica. PhD Thesis, Instituto de Geociências, Universidade de São Paulo, 212 p. DOI: 10.11606/T.44.2016.tde-24062016-160651

Assis R.R., Xavier R.P., Creaser R.A. 2017. Linking the timing of disseminated granite- hosted gold-rich deposits to paleoproterozoic felsic magmatism at alta floresta gold province, Amazon Craton, Brazil: Insights from pyrite and molybdenite Re-Os geochronology. Economic Geology, 112, 1937–1957. https://doi.org/10.5382/ econgeo.2017.4535

Barros M.A.S., Chemale Júnior F., Nardi L.V.S., Lima E.F. 2009. Paleoproterozoic bimodal post-collisional magmatism in the southwestern Amazonian Craton, Mato Grosso, Brazil: geochemistry and isotopic evidence. Journal of South American Earth Sciences, 27, 11–23. https://doi.org/10.1016/j.jsames.2008.11.003

Betiollo L.M., Reis N.J., Almeida M.E., Bahia R.B.C., Splendor F., Costa U.A.P., Luzardo R. 2009. Magmatismo Máfico Calimiano (Sill Mata-Matá). rio Aripuanã. Amazonas – Implicações Geológicas. In: Simpósio de Geologia da Amazônia, Manaus, AM., 11, 162. Available on line at: https://sbg-no.org.br/arquivos/BASES/Anais%2011%20Simp%20Geol%20Amaz%20Agosto-2005-Manaus.pdf / (accessed on 10 November 2022)

Bettencourt J.S., Leite W.B. Jr., Ruiz A.S., Matos M., Payolla B.L., Tosdal R.M. 2010. The Rondonian-San Ignacio Province in the SW Amazonian Craton: An overview. Journal of South American Earth Sciences, 29, 28-46. https://doi.org/10.1016/j.jsames.2009.08.006

Bettencourt J.S., Tosdal R.M., Leite Júnior W.B., Payolla B.L. 1999. Mesoproterozoic rapakivi granites of the Rondônia Tin Province, southwestern border of the Amazonian Craton, Brazil: reconnaissance U–Pb geochronology and regional implications. Precambrian Research, 95, 41-67. https://doi.org/10.1016/S0301-9268(98)00126-0

Bini E.G., Barros M.A.S., Pierosan R., Santos J.O.S. 2015. Petrography and geochronology of felsic volcanic rocks at the eastern portion of Serra do Cachimbo, southcentral Amazonian Craton, Brazil. In: Simposio de Vulcanismo e Ambientes, 6, 67. Available on line at: http://sbg.sitepessoal.com/anais_digitalizados/vulcanismo/vulcanimo%202015.pdf / (accessed on 10 November 2022)

Bispo-Santos F., D´Agrella-Filho M.S., Trindade R.I.F., Janikian L., Reis N.J. 2014. Was there SAMBA in Columbia? Paleomagnetic evidence from 1790 Ma Avanaveiro mafic sills (Northern Amazonian craton). Precambrian Research, 244, 139-155. https://doi.org/10.1016/j.precamres.2013.11.002

Bispo-Santos F., D'Agrella-Filho M.S., Pacca I.I.G., Janikian L., Trindade R.I.F., Elming, S.G.Å., Silva J.A., Barros M.A.S., Pinho F.E.C. 2008. Columbia revisited: Paleomagnetic results from the 1790 Ma Colider volcanics (SW Amazonian Craton, Brazil). Precambrian Research, 164, 40-49. https://doi.org/10.1016/j.precamres.2008.03.004

Bispo-Santos F., D´Agrela-Filho M.S., Pesonen L.J., Salminen J.M., Reis N.J., Silva J.M. 2020. The long life of SAMBA connection in Columbia: A paleomagnetic study of the 1535 Ma Mucajaí Complex, northern Amazonian Craton, Brazil. Gondwana Research, 80, 285-302. https://doi.org/10.1016/j.gr.2019.09.016

Brito R.S., Silva M.S., Silveira F.V., Larizzati J.H., Chemale Júnior F. 2008. Dados preliminares de litogeoquímica, U-Pb-ICP-MS laser ablation, Sm-Nd e Sr-Sr das rochas encaixantes das mineralizações de ouro do garimpo Eldorado do Juma-Amazonas. In: Congresso Brasileiro de Geologia, 44, 94. Available on line at: https://rigeo.cprm.gov.br/handle/doc/729 / (accessed on 10 November 2022)

Brito R.S., Silveira F.V., Larizzati J.H. 2010. Metalogenia do distrito aurífero do rio Juma-Nova Aripuanã, AM. Manaus: CPRM. 43 p. (Informe de Recursos Minerais. Série Ouro. Informes Gerais, 17). Available on line at: https://rigeo.cprm.gov.br/handle/doc/1753 / (accessed on 10 November 2022)

Bühn B., Pimentel M.M., Matteini M., Dantas E.L. 2009. High spatial resolution analysis of Pb and U isotopes for geochronology by laser ablation multi-collector inductively coupled plasa ass spectroetry (L-C-ICPMS). Anais da Academia Brasileira de Ciências, 81, 99-114. https://doi.org/10.1590/S0001-37652009000100011

Carneiro C.D.C., Juliani C., Carreiro-Araujo S.A., Monteiro L.V.S., Crosta A.P., Fernandes C.M.D. 2018. New crustal framework in the amazon craton based on geophysical data: evidences of deep east-west trending suture zones. IEEE Geoscience Remote Sensing Letters, 16, 20–24. https://doi.org/10.1109/LGRS.2018.2867551

Collins W.J. 2002. Hot orogens, tectonic switching, and creation of continental crust. Geology, 30, 535–538. https://doi.org/10.1130/0091-7613(2002)030<0535:HOTSAC>2.0.CO;2

Compston W., Williams I.S., Kirschvink J.L., Zichao Z., Guogan M. 1992. Zircon ages for the Early Cambrian time-scale. Journal of Geological Society, 149, 171-184. https://doi.org/10.1144/gsjgs.149.2.0171

Compston W., Williams I.S., Meyer C. 1984. Geochronology of zircons from the lunar breccia 73217 using a sensitive high mass resolution ion microprobe. Journal of Geophysical Research, 89, 525-534. https://doi.org/10.1029/JB089iS02p0B525

Cordani U.G., Brito Neves B. 1982. The geologic evolution of south america during the Archean and early Proterozoic. Revista Brasileira de Geociências, 12, 78–88. Available on line at: https://www.ppegeo.igc.usp.br/index.php/rbg/article/view/12193 / (accessed on 17 November 2022).

Cordani U.G., Teixeira W. 2007. Proterozoic accretionary belts in the amazonian craton. Geological Society of America, Memoir Geological Society of America, 200, 297–320. https://doi.org/10.1130/2007.1200(14)

D´Agrella-Filho M.S., Santos F.B., Trindade R.I.F., Antonio P.Y.J. 2016. Paleomagnetism of the Amazonian Craton and its role in paleocontinents. Brazilian Journal of Geology, 46 (2), 275-299. DOI: 10.1590/2317-4889201620160055

Dezula S.E.M, Barros M.A.S., Pierosan R., Santos J.O.S., Assis R.R. 2018. Granito Aragão - Suíte intrusiva Nhandú - um granito oxidado, tipo A2, de 1967 a 1964 Ma na Província Aurífera Alta Floresta - Cráton Amazônico. Boletim de Geologia da USP, Série Científica, 18 (1), 3-20. https://doi.org/10.11606/issn.2316-9095.v18-434

Diener F.S., Polo H.J.O., Carneiro J.S.M. 2019. Geologia e recursos minerais da folha Rio Branco - SC.20-Z-B, estado do Mato Grosso. Goiânia, CPRM. Available on line at: https://rigeo.cprm.gov.br/handle/doc/21297 / (accessed on 17 November 2022).

Duarte T.B. 2015. Geologia, geoquimica e geocronologia do dominio vulcanico do arco magmatico Juruena, SW do Cráton Amazônico: implicações geotectônicas. M.Sc. Dissertation, Instituto de Geociências, Universidade de Campinas, 124 p. Available on line at: https://rigeo.cprm.gov.br/handle/doc/14780 / (accessed on 17 November 2022).

Duarte T.B., Rodrigues J.B., Ribeiro P.S.E., Scandolara J.E. 2012. Tectonic evolution of the Juruena magmatic arc between the Aripuanã and Juruena rivers: northwest Mato Grosso State, Brazil. Brazilian Journal of Geology, 42 (4), 824-840. Available on line at: https://ppegeo.igc.usp.br/index.php/rbg/article/view/7973 / (accessed on 17 November 2022).

Duarte T.B., Xavier R., Rodrigues J. 2019. A review of the geodynamic setting of the Volcanic Domain in the Juruena Magmatic Arc, southwestern Amazon Craton, Brazil, based on geochemical, U-Pb and Sm-Nd data. Journal of the Geological Survey of Brazil, 2, 37–73. https://doi.org/10.29396/jgsb.2019.v2.n1.4

Fernandes C.M.D., Juliani C. 2019. The tectonic controls on the Paleoproterozoic volcanism and the associated metallogeny in the South Amazonian craton, Brazil: Sr–Nd–Pb isotope constraints. Precambrian Research, 331, 105354. https://doi.org/10.1016/j.precamres.2019.105354

Frasca A.A.S., Borges F.R. (org.). 2005. Geologia e Recursos Minerais da Folha Ilha 24 de Maio - SC.21-Z-A - Estado de Mato. Programa Levantamentos Geológicos Básicos do Brasil - PLGB. Projeto Província Mineral de Alta Floresta (PROMIN Alta Floresta). Brasilia: CPRM.

Geraldes M.C., Van Schmus W.R., Condie K.C., Bell S., Teixeira W., Babinski M. 2001. Proterozoic Geologic Evolution of the SW Part of the

Amazonian craton in Mato Grosso State. Brazil. Precambrian Research, 111, 91-108. https://doi.org/10.1016/S0301-9268(01)00158-9

Gower C.F., Krogh T.E. 2002. A U-Pb geochronological review of the Proterozoic history of the eastern Grenville Province. Canadian Journal of Earth Sciences, 39 (5), 795-829. https://doi.org/10.1139/e01-090

Grove M., Harrison T.M. 1996. 40Ar diffusion in Fe-rich biotite. American Mineralogist, 81, 940-951. https://doi.org/10.2138/am-1996-7-816

Heaman L.M. 2009. The application of U–Pb geochronology to mafic, ultramafic and alkaline rocks: An evaluation of three mineral standards. Chemical Geology, 261, 42-51. https://doi.org/10.1016/j.chemgeo.2008.10.021

Heaman L.M., Gower C.F., Perreault S. 2004. The timing of Proterozoic magmatism in the Pinware terrane of southeast Labrador, easternmost Quebec and northwest Newfoundland. Canadian Journal of Earth Sciences, 41 (2), 127-150. https://doi.org/10.1139/e03-088

Högdahl K., Andersson U.B., Eklund O. 2004. The transscandinavian igneous belt (TIB) in Sweden: a review of its character and evalution. Geological Survey of Finland, Special Paper 37, 123 p.

JICA; MMAJ. 2000. Final Report. Report on the mineral exploration in the Alta Floresta area, Federative Republic of Brazil. Japan International Cooperation Agency. Metal Mining Agency of Japan. 137p.

Johansson Å. 2009. Baltica, Amazonia and the SAMBA connection – 1000 million years of neighbourhood during the Proterozoic? Precambrian Research, 175, 221-234. https://doi.org/10.1016/j.precamres.2009.09.011

Johansson Å. 2021. Cleaning up the record – revised U-Pb zircon ages and new Hf isotope data from southern Sweden. GFF 143, 32 pp. https://doi.org/10.1080/11035897.2021.1939777

Kamber B.S., Kramers J.D., Napier R., Cliff R.A., Rollinson H.R. 1995. The Triangle Shear Zone, Zimbabwe, revisited: new data document an important event at 2.0 Ga in the Limpopo Belt. Precambrian Research, 70, 191-213. https://doi.org/10.1016/0301-9268(94)00039-T

Kirschner D.L., Cosca M.A., Masson H., Hunziker J.C. 1996a. Staircase 40Ar/39Ar spectra of fine-grained white mica: timing and duration of deformation and empirical constraints on argon diffusion. Geology, 24, 747–750. https://doi.org/10.1130/0091-7613(1996)024<0747:SAASOF>2.3.CO;2

Kirschner D.L., Hunziker J.C., Cosca M. 1996b. Closure temperature of argon in micas, a review and reevaluation based on Alpine samples. Geological Society of America, Abstracts with Programs, 28, 441.

Klein E., Almeida M.E., Rosa-Costa L.T. 2012. The 1.89-1.87 Ga Uatumã Silicic Large Igneous Province, northern South America. In: International Association of Volcanology and Chemistry of the Earth's Interior, Large Igneous Province Commission, November. LIP of the month. Available on line at: http://www.largeigneousprovinces.org/12nov / (accessed on 17 November 2022).

Knust S.S.A. 2010. Geologia e recursos minerais da Folha Porto dos Gaúchos. Goiânia, CPRM. 141 p. Projeto Noroeste-Nordeste do Mato Grosso. Programa Geologia do Brasil – PGB. Available on line at: https://rigeo.cprm.gov.br/handle/doc/11201 / (accessed on 17 November 2022).

Leal J.W.L., Silva G.F., Santos D.B. dos, Teixeira W., Lima M.I.C., Fernandes A.C., Pinto A.C. 1978. Geologia. In: Folha SC 20 Porto Velho: geologia, geomorfologia, pedologia, vegetação, uso potencial da terra. Rio de Janeiro. Projeto RADAMBRASIL, Levantamento de Recursos Naturais, 16, 17-184. Available on line at: https://biblioteca.ibge.gov.br/biblioteca-catalogo.html?id=224033&view=detalhes / (accessed on 17 November 2022).

Lee J.Y., Marti K., Severinghaus J.P., Kawamura K., Yoo. H.S., Lee J.B., Kim J.S. 2006. A redetermination of the isotopic abundances of atmospheric Ar. Geochimica et Cosmochimica Acta, 70, 4507-4512. https://doi.org/10.1016/j.gca.2006.06.1563

Leite J.A.D., Souza M.Z.A., Saes G.S., Batata M.E., Oliveira F.A., Menezes T., Freitas F.A.O. Gomes M.F., Uchôa J., Silva V.F., Silva D.R. 2006. Geologia, geocronologia e evolução crustal de partes da porção sul do Cráton Amazônico no Alto Estrutural Eugênia-Arinos, médio-noroeste de Mato Grosso. In: Viana R.R., Fernandes C.J. (coord.). Coletâneas Geológicas do estado de Mato Grosso: Geologia Regional. Cuiabá, EDUFMT-Lenice,1, 61-76.

Lisboa T.M. 2019. Metamorfismo de alta T e média P de paragnaisses, anfibolitos e hornblenda-biotita gnaisse do Complexo Quatro Cachoeiras, Província Rondônia-Juruena, Rio Guariba, Amazonas. M.Sc. Dissertation, Universidade Federal do Amazonas, 117p. https://tede.ufam.edu.br/handle/tede/7663

Ludwig K.R. 2001. SQUID 1.02: User Manual - A Geochronological Toolkit for Microsoft Excel. Berkeley: Berkeley Geochronology Center Special Publication.

Ludwig K.R. 2003. Isoplot 3.00: A geochronological toolkit for Microsoft Excel. Berkeley Geochronology Center, Berkeley, 70.

Mark D.F., Stuart F.M., Podesta M. 2011. New high-precision measurements of the isotopic composition of atmospheric argon. Geochimica et Cosmochimica Acta, 75, 7494-7501. https://doi.org/10.1016/j.gca.2011.09.042

Martins E.G., Abdallah S. 2007. Geologia e recursos minerais da folha Juína SC.21-Y-C. Goiânia: CPRM. Escala 1:250.000. Programa Geologia do Brasil - PGB; Projeto Noroeste de Mato Grosso. Available on line at: https://rigeo.cprm.gov.br/handle/doc/10281/ (accessed on 17 November 2022).

Meloni R.E., Simões M.S., Oliveira A.C.S. (org.). 2021. Áreas de relevante interesse mineral (ARIM): evolução crustal e metalogenia do sudeste do Amazonas: distrito aurífero Juma, estado do Amazonas. Manaus, SGB-CPRM. Informe de Recursos Minerais. Série Províncias Minerais do Brasil, 34. Available on line at: https://rigeo.cprm.gov.br/handle/doc/22194 / (accessed on 10 November 2022)

Miller J.S., Matzel J.E.P., Miller C.F., Burgess S.D., Miller, R.B. 2007. Zircon growth and recycling during the assembly of large, composite arc plutons. Journal of Volcanology and Geothermal Research, 167, 282–299. https://doi.org/10.1016/j.jvolgeores.2007.04.019

Motta J.G., Betts P.G., Meira V.T., Trevisan V.G., de Souza Filho C.R. 2022. Unwrapping reworked crust at the Columbia supercontinent margin within central southern Amazon Craton using multi-source geophysics and geochronology data synergy. Geoscience Frontiers, 13, 101348. https://doi.org/10.1016/j.gsf.2022.101348

Moura M.A. 1998. O maciço granítico Matupá no depósito de ouro Serrinha (MT): petrologia, alteração hidrotermal e metalogenia. PhD Thesis, Universidade de Brasília, 238 p. Available on line at: https://repositorio.unb.br/handle/10482/8040 / (accessed on 10 November 2022)

Neder R.D., Leite J.A.D., Figueiredo B.R., Mcnaugton N.J. 2002. 1.76 Ga volcanoplutonism in the southwestern Amazonian Craton, Aripuanã-MT, Brazil: tectono-stratigraphic implications from SHRIMP U–Pb zircon data and rock geochemistry. Precambrian Research, 119 (1-4), 171-187. https://doi.org/10.1016/S0301-9268(02)00122-5

Neder R.D., Figueiredo B.R., Beaudry C., Collins C., Leite J.A.D. 2000. The expedito massive sulfide deposit, Mato Grosso. Revista Brasileira de Geociências, 30, 222–225. https://doi.org/10.25249/0375-7536.2000302222225

Oliveira A.C.S. 2016. Evolução tectônica do Craton Amazonas na região Sudeste do estado do Amazonas: um estudo em múltiplas escalas com base na integração de dados geológico–estruturais e geofísicos. M.Sc. Dissertation, Universidade Federal do Amazonas, Manus, 64 p. Available on line at: https://tede.ufam.edu.br/handle/tede/5158 / (accessed on 10 November 2022)

Oliveira A.C.S., Lira R.R.C. 2019. Geologia e recursos minerais da folha Rio Roosevelt - SB.20-X-B, estados do Amazonas. Manaus, CPRM. 57 p. Escala 1:250.000. Available on line at: https://rigeo.cprm.gov.br/handle/doc/21319 / (accessed on 10 November 2022)

Oliveira A.C.S., Almeida M.E. 2021. The role of intracratonic crustal reworking in the tectonic compartmentalization of the Juruena Terrane, SW Amazonas Craton: the Roosevelt-Guariba Transpressive Belt. Journal of the Geological Survey of Brazil, 4 (2), 123-145. https://doi.org/10.29396/jgsb

Payolla B. L., Kozuch M., Leite Junior W.B., Bettencourt J.S., Van Schmus W.R. 1998. Novas idades U-Pb em zircões de gnaisses e granitóides da região de Ariquemes, estado de Rondônia: implicações para a evolução geológica da borda sudoeste do cráton Amazônico. In: Congresso Brasileiro de geologia, 40, 39. Available on line at: http://sbg.sitepessoal.com/anais_digitalizados/1998-BELO%20HORIZONTE/CBG1998.pdf / (accessed on 10 November 2022)

Payolla B.L., Bettencourt J.S., Kozuch M., Leite Júnior W.B., Fetter A.H., Van Schmus W.R. 2002. Geological evolution of the basement rocks in the east-central part of the Rondônia Tin Province, SW Amazonian Craton. Brazil: U-Pb and Sm-Nd isotopic constraints. Precambrian Research, 119, 141-169. https://doi.org/10.1016/S0301-9268(02)00121-3

Payolla B.L., Bettencourt J.S., Tosdal R.M., Wooden J.L., Leite Júnior W.B. 2003a. SHRIMP U-Pb zircon geochronology of high-grade paragneiss from NE Rondônia. SW Amazonian Craton. Brazil: constraints of provenance and metamorphism. In: South American Symposium on

Isotope Geology, 4., 248-251. Available on line at: https://horizon.documentation.ird.fr/exl-doc/pleins_textes/divers17-05/010039206.pdf / (accessed on 10 November 2022)

Payolla B.L., Fetter A.H., Bettencourt J.S., Leite Júnior W.B. 2003b. U-Pb monazite ages from pelitic paragneisses in the NE Rondônia. SW Amazonian Craton: evidence for 1.54 Ga metamorphism. In: South American Symposium on Isotope Geology, 4., 244-247. Available on line at: https://horizon.documentation.ird.fr/exl-doc/pleins_textes/divers17-05/010039206.pdf / (accessed on 10 November 2022)

Pesonen L.J., Mertanen S., Veikkolainen T. 2012. Paleo-Mesoproterozoic Supercontinents – a paleomagnetic view. Geophysica, 47, 5-47. Available on line at:https://www.geophysica.fi/pdf/geophysica_2012_48_pesonen.pdf / (accessed on 10 November 2022)

Pimentel M.M. 2001. Resultados geocronológicos do Projeto PROMIN Alta Floresta. Brasília, University of Brasília. Internal Report.

Pinho M.A.S.B. 2002. Geoquímica e geocronologia da sequência volcano-plutônica Teles Pires, norte do Mato Grosso. In: Congresso Brasileiro de Geologia, 41., João Pessoa, 465. Available on line at: http://sbg.sitepessoal.com/anais_digitalizados/2002-JOAO%20PESSOA/2002-JO%C3%83O%20PESSOA.pdf / (accessed on 10 November 2022)

Pinho M.A.S.B., Van Schums W.R., Chemale Jr. F., Pinho. F.E.C. 2003. U-Pb and Sm-Nd evidence for 1.78 Ga magmatism in the Moriru Region., Mato Grosso. Brasil: implications for province boundaries in the Amazon Craton. Precambrian Research, 126, 1-25. https://doi.org/10.1016/S0301-9268(03)00126-8

Pinho M.A.S.B., Lima E.F., Fetter A., Van Schmus W.R., Chemale Jr. F. 2001. Caracterização petrografica e dados geocronologicos preliminares das rochas vulcanicas da formação Iriri – Porção Centro-Sul do Craton Amazônico, Aripuanã, Mato Grosso. Revista Brasileira de Geociências, 31, 1-5. Available on line at: https://ppegeo.igc.usp.br/index.php/rbg/article/view/10442 / (accessed on 10 November 2022)

Prado S.E, Barros M.A.S., Pinh, F.E.C, Pierosan, R. 2013. Granito Terra Nova – petrologia e geocronologia: um granito tipo-A da Província Alta Floresta – Craton Amazônico. Brazilian Journal of Geology, 43 (1), 101-116. http://dx.doi.org/10.5327/Z2317-48892013000100009

Purdy J., Jäger E. 1976. K-Ar ages on rock forming minerals from the Central Alps. Memorie degli Istituti di Geologia e Mineralogia dell' Universita di Padova, 30, 3-31.

Quadros M.L.E.S., Palmeira L.C.M., Castro C.C. 2011. Geologia e recursos minerais da folha Rio Machadinho (SC.20-X-C). Porto Velho, CPRM. Escala 1:250.000. Available on line at: https://rigeo.cprm.gov.br/handle/doc/11360 / (accessed on 10 November 2022)

Quadros M.L.E.S., Rizzotto G.J. (org.). 2007. Geologia e recursos minerais do estado de Rondônia: texto explicativo do mapa geológico e de recursos minerais do estado de Rondônia. Porto Velho; Rondônia: CPRM. Escala 1:1.000.000. Programa Geologia do Brasil (PGB). Available on line at: https://rigeo.cprm.gov.br/handle/doc/10277 / (accessed on 10 November 2022)

Reis N.J., Bahia R.B.C., Almeida M.E., Costa U.A.P., Betiollo L.M., Oliveira A.C., Splendor F. 2013. O Supergrupo Sumaúma no contexto geológico da Folha SB.20-Z-D (Sumaúma), sudeste do Amazonas: modo de ocorrência, discussão de idades em zircões detríticos e correlações no SW do Cráton do Amazonas. In: Wankler F.L., Holanda E.S., Vasquez M.L. (eds.). Contribuições à geologia da Amazônia. Belém, Sociedade Brasileira de Geologia Núcleo Norte (SBG-NO), 8, 197- 222. Available on line at: https://sbg-no.org.br/arquivos/BASES/CGA%208.pdf / (accessed on 10 November 2022)

Reis N.J., Oliveira A.C.S., Oliveira A.A., Bahia R.B.C. 2017. Geologia e recursos minerais da Folha Mutum – SB.20-Z-B, Estado do Amazonas, escala 1:250.000. Manaus: CPRM. Available on line at: https://rigeo.cprm.gov.br/handle/doc/17804 / (accessed on 10 November 2022)

Reis, N.J., Almeida, M.E., Riker, S.R., Ferreira, A.L. (org.). 2006. Geologia e recursos minerais do estado do Amazonas. Manaus, CPRM; CIAMA. Available on line at: https://rigeo.cprm.gov.br/handle/doc/2967 / (accessed on 10 November 2022)

Renne P.R., Balco G., Ludwig R.L., Mundil R., Min K. 2011. Response to the comment by W.H. Schwarz et al. on "Joint determination of 40K decay constants and 40Ar*/40K for the Fish Canyon sanidine standard. and improved accuracy for 40Ar/39Ar geochronology" by 782 Koenraad de Jong, Gilles Ruffet, P.R. Renne et al. (2010). Geochimica et Cosmochimica Acta, 75, 5097-5100. https://doi.org/10.1016/j.gca.2011.06.021

Ribeiro P.S.E., Duarte T.B. (org.). 2010. Geologia e recursos minerais das folhas Rio Guariba SC.20-X-D e Rio Aripuanã SC.21-V.C: escala 1:250.000. Goiânia: CPRM, 2010. Available on line at: https://rigeo.cprm.gov.br/handle/doc/11355/ (accessed on 10 November 2022)

Rizzotto G.J., Alves C.L., Rios F.S., Barros M.A.S. 2019a. The Nova Monte Verde metamorphic core complex: tectonic implications for the southern Amazonian craton. Journal of South American Earth Sciences, 91, 154–172. https://doi.org/10.1016/j. jsames.2019.01.003

Rizzotto G.J., Alves C.L., Rios F.S., Barros, M.A.S. 2019b. The Western Amazonia Igneous Belt. Journal of South American Earth Sciences, 96, 102326. https://doi.org/10.1016/j.jsames.2019.102326

Rizzotto G.J., Quadros M.L.E.S., Oliveira J.G. de, Castro J.M., Lafon J.M. 2006. Idades Pb-evaporação dos granitos do setor noroeste do Estado de Rondônia. In: Simpósio de Geologia da Amazônia, 9, 2006, Belém. Available on line at: https://sbg-no.org.br/arquivos/BASES/Anais%209%20Simp%20Geol%20Amaz%20Marco-2006-Belem.pdf / (accessed on 10 November 2022)

Rizzotto G.J., Quadros M.L.E.S., Silva L.C., Armstrong R., Almeida M.E. 2002. O Granito Aripuanã: Datação U-Pb (SHRIMP) e Implicações Metalogenéticas. In: Congresso Brasileiro de Geologia, 41, João Pessoa. p. 469. Available on line at: http://sbg.sitepessoal.com/anais_digitalizados/2002-JOAO%20PESSOA/2002-JO%C3%83O%20PESSOA.pdf / (accessed on 10 November 2022)

Rocha M.L.B.P., Chemale Jr F., Santos J.O.S., Barros M.A.S., Pinho F.E.C., McNaughton N.J., Costa P.C.C., Roberts M. 2020. U-Th-Pb Shrimp dating of hydrothermal monazite from the Trairão Gold Deposit - Alta Floresta Gold Province (Amazon Craton). Brazilian Journal of Geology, 50 (1), 20190063. https://doi.org/10.1590/2317-4889202020190063

Roverato M., Giordano D., Giovanardi T., Juliani C., Polo L. 2019. The 2.0–1.88 Ga Paleoproterozoic evolution of the southern Amazonian Craton (Brazil): An interpretation inferred by lithofaciological, geochemical and geochronological data. Gondwana Research, 70, 1-24. https://doi.org/10.1016/j.gr.2018.12.005

Roverato M., Juliani C., Fernandes C.M.D., Capra L. 2017. Paleoproterozoic andesitic volcanism in the southern Amazonian craton, the Sobreiro Formation: new insights from lithofacies analysis of the volcaniclastic sequences. Precambrian Research, 289, 18-30. https://doi.org/10.1016/j.precamres.2016.11.005

Ruffet G., Feraud G., Amouric M. 1991. Comparison of 39Ar-40Ar conventional and laser dating of biotites from the North Tregor Batholith. Geochimica et Cosmochimica Acta, 55, 1675-1688. https://doi.org/10.1016/0016-7037(91)90138-U

Ruffet G., Féraud G., Balèvre M., Kiénast J.-R. 1995. Plateau ages and excess argon in phengites: an 40Ar–39Ar laser probe study of Alpine micas (Sesia Zone.Western Alps. northern Italy). Chemical Geology (Isotopic Geoscience Section) 121, 327–343. https://doi.org/10.1016/0009-2541(94)00132-R

Salminen J.M., Evans D.A.D., Trindade R.I.F., Smirnov A.V. 2016. Paleogeography of the Congo/São Francisco craton at 1.5 Ga: expanding the core of Nuna supercontinent. Precambrian Research, 286, 195-212. https://doi.org/10.1016/j.precamres.2016.09.011

Santos F.S., Pierosan R., Barros M.A.S., Geraldes M.C., Lima M.F. 2019. Petrology of the Colíder Group volcanics successions in the northernmost Mato Grosso, Brazil: A contribution to the knowledge of the felsic volcanism of the Alta Floresta Gold Province. Journal of South American Earth Sciences, 89, 10-29. https://doi.org/10.1016/j.jsames.2018.10.007

Santos J.O.S. 2003. Geotectônica dos Escudos das Guianas e Brasil Central. In: Bizzi L.A., Schobbenhaus C., Vidotti R.M., Gonçalves J.H. (eds.). Geologia, tectônica e recursos minerais do brasil: texto, mapas e SIG. Brasília, CPRM. cap. 4, p. 169-226. Available on line at: https://rigeo.cprm.gov.br/handle/doc/5006 / (accessed on 10 November 2022)

Santos J.O.S., Hartmann L.A., Gaudette H.E., Groves D.I., Mcnaughton N.J., Fletcher I.R. 2000. A new understanding of the provinces of the Amazonian Craton based on integration of field mapping and U-Pb and Sm-Nd geochronology. Gondwana Research, 3, 453-488. https://doi.org/10.1016/S1342-937X(05)70755-3

Santos J.O.S., Rizzotto G.J., Chemale Jr. F., Hartmann L.A., Quadros M.L.E.S., Mcnaughton N.J. 2003. Three distinctive colisional orogenies in the southwestern Amazon Craton: constraints from U-Pb geochronololgy. In: South American Symposium on Isotope Geology, 4, Salvador, 282-285. Available on line at: https://rigeo.cprm.gov.br/handle/doc/464 / (accessed on 10 November 2022)

Santos J.O.S., Rizzotto G.J., Potter P.E., McNaughton N.J., Matos R.S., Hartmann L.A., Chemale Jr F., Quadros M.L.E.S. 2008. Age and autochthonous evolution of the Sunsás Orogen in West Amazon Craton

based on mapping and U–Pb geochronology. Precambriam Research, 165, 120–152. https://doi.org/10.1016/j.precamres.2008.06.009

Scandolara J.E. 2006. Geologia e evolução do terreno Jamari, embasamento da faixa Sunsas/Aguapeí, centro-leste de Rondônia, sudoeste do Cráton Amazônico. PhD Thesis, Universidade de Brasília, 462 p. Available on line at: https://repositorio.unb.br/handle/10482/2498 / (accessed on 10 November 2022)

Scandolara J.E., Correa R.T., Fuck R.A., Souza V.S., Rodrigues J.B., Ribeiro P.S.E., Frasca A.A.S., Saboia A.M., Lacerda Filho J.V. 2016. Paleo-Mesoproterozoic arc-accretion along the southwestern margin of the Amazonian craton: The Juruena accretionary orogen and possible implications for Columbia supercontinent. Journal of South American Earth Sciences, 73, 223–247. https://doi.org/10.1016/j.jsames.2016.12.005

Scandolara J.E., Fuck R.A., Dall'Agnol R., Dantas E.L. 2013. Geochemistry and origin of the early Mesoproterozoic mangerite–charnockite–rapakivi granite association of the Serra da Providência suite and associated gabbros, central–eastern Rondônia, SW Amazonian Craton, Brazil. Journal of South American Earth Sciences, 45, 166–193. https://doi.org/10.1016/j.jsames.2013.03.003

Scandolara J.E., Ribeiro P.S.E., Frasca. A.A.S., Fuck R.A., Rodrigues J.B. 2014. Geochemistry and geochronology of mafic rocks from the Vespor suite in the Juruena arc. Roosevelt-Juruena terrain. Brazil: implications for Proterozoic crustal growth and geodynamic setting of the SW Amazonian craton. Journal of South American Earth Sciences, 53, 20-49. https://doi.org/10.1016/j.jsames.2014.04.001

Scandolara J.E., Ribeiro P.S.E., Quadros M.L.E.S., Duarte T.B., Frasca A.A.S. 2011. O arco magmático Juruena-Jamari: uma entidade geotectônica Paleoproterozóica única no SW do Cráton Amazônico? In: Simpósio de Geologia da Amazônia, 12, 190-193. Available on line at: https://sbg-no.org.br/arquivos/BASES/Anais%2012%20Simp%20Geol%20Boa%20Vista%20Outubro-2011.pdf / (accessed on 10 November 2022)

Scandolara J.E., Rizzotto G.J., Bahia R.B.C., Quadros M.L.E.S., Amorim J.L., Dall'Igna L.G., 1999. Geologia e recursos minerais do estado de Rondônia: texto explicativo e mapa do estado de Rondônia. Brasília, CPRM. Escala 1:1.000.000. Programa Levantamentos Geológicos do Brasil - PLGB. Available on line at: https://rigeo.cprm.gov.br/handle/doc/2419 / (accessed on 10 November 2022)

Siivola J., Schmid R. 2007. List of mineral abbreviations. IUGS Subcommission on the Systematics of Metamorphic Rocks. Web version 01.02.07. Available on line at: http://www.ngdc.nerc.ac.uk/scmr/docs/papers/paper_12.pdf / (accessed on 10 November 2022)

Silva F.R., Barros M.A.S., Moura M.A., Pierosan R., Santos J.O.S., Oliveira D.R.P. 2015. Petrografia, química mineral e geocronologia U-Pb dos granitos da região de Guarantã do Norte, MT: evidências de mistura de magmas. In: Simpósio de Geologia do Centro-Oeste, 14, Brasília, p. 199-201. Available on line at: http://sbg.sitepessoal.com/anais_digitalizados/simposiocentrooeste/2015.pdf / (accessed on 10 November 2022)

Silva F.R., Barros M.A.S., Pierosan R., Pinho F.E.C., Rocha M.L.B.P., Vasconcelos B.R, Dezula S.E.M., Tavares C., Rocha J. 2014. Geoquímica e geocronologia U-Pb (SHRIMP) de granitos da região de Peixoto de Azevedo: Província Aurífera Alta Floresta, Mato Grosso. Brazilian Journal of Geology, 44(3), 433-455. http://dx.doi.org/10.5327/Z2317-4889201400030007

Silva F.R., Pierosan R., Barros M.A.S., Moura M.A., Santos F.S. 2018. Geocronologia de granitos da região de Guarantã do Norte (MT) – craton Amazonico – Brasil. In: Congresso Brasileiro de Geologia, 49, Rio de Janeiro-RJ. Available on line at: http://cbg2018anais.siteoficial.ws/resumos/9316.pdf / (accessed on 10 November 2022)

Silva L.C., Armstrong, R., Pimentel M.M., Scandolara J., Ramgrab G., Wildner W., Angelim L.A.A., Vasconcelos A.M., Rizzoto G.J., Quadros M.L.E.S., Sander A., De Rosa A.L.Z. 2002. Reavaliação da evolução geológica em terrenos Pré-Cambrianos brasileiros com base em novos dados U-Pb SHRIMP, Parte III: Províncias Borborema, Mantiqueira Meridional e Rio Negro-Juruena. Revista Brasileira de Geociências, 32 (4), 529–544. Available on line at: https://ppegeo.igc.usp.br/index.php/rbg/article/view/9846 / (accessed on 10 November 2022).

Silva M.G., Abram M.B. (org.). 2008. Projeto Metalogenia da Província Aurífera Juruena-Teles Pires, Mato Grosso. Goiânia, CPRM. 212 p. (Informe de Recursos Minerais. Série Ouro, 16). Available on line at: https://rigeo.cprm.gov.br/handle/doc/1745 / (accessed on 10 November 2022)

Simões M.S., Meloni R.E., Santos J.O.S. 2020. Stratigraphy, depositional environments and zircon U-Pb (LA-ICP-MS) ages of the Statherian volcano-sedimentary Beneficente Group: implications for tectonics and gold mineralization in SW of the Amazon Craton. Precambrian Research, 345, 105756. https://doi.org/10.1016/j.precamres.2020.105756

Smith J.B., Barley M.E., Groves D.I., Krapez B., McNaughton N.J., Bickle J., Chapman H.J. 1998. The Scholl Shear Zone, West Pilbara: evidence for a domain boundary structure from integrated tectonostratigraphic analyses, SHRIMP U-Pb dating and isotopic and geochemical data of granitoids. Precambrian Research, 88, 143-171. https://doi.org/10.1016/S0301-9268(97)00067-3

Souza J.O., Abreu F.W. (org.). 2007. Geologia e recursos minerais da folha Tapaiuna SC.21-Y-B: escala 1:250.000. Goiânia: CPRM. Programa Geologia do Brasil (PGB); Projeto Noroeste de Mato Grosso. Available on line at: https://rigeo.cprm.gov.br/handle/doc/10282/ (accessed on 10 November 2022)

Souza J.O., Frasca A.A.S., Oliveira C.C. 2005. Geologia e recursos minerais da folha Alta Floresta (relatório integrado): folhas SC.21-X-C, SC.21-V-D, SC.21-Z-A e SC.21-Z-B: estados de Mato Grosso e do Pará. Brasília, CPRM. Programa Levantamentos Geológicos Básicos do Brasil - PLGB; Projeto Província Mineral de Alta Floresta (PROMIN-Alta Floresta). Available on line at: https://rigeo.cprm.gov.br/handle/doc/10246 / (accessed on 10 November 2022)

Stephens M.B., Bergman W.J. (eds.). 2020. Sweden: lithotectonic framework, tectonic evolution and mineral resources. Geological Society Memoir 50, Geological Society of London, 631p. https://doi.org/10.1144/M50

Stern R.A. 2001. A new isotopic and trace-element standard for the ion microprobe: preliminary thermal ionization mass spectrometry (TIMS) U-Pb and electron-microprobe data: in radiogenic age and isotopic studies. Geological Survey of Canada, Current Research 2001-F1, 11 p.

Tassinari C.C.G., Bettencourt J.S., Geraldes M.J.B., Macambira M.J.B., Lafon J.M. 2000. The Amazonian craton. In: Cordani U.G., Milani E.J., Thomaz Filho A., Campos D.A. (eds.). Tectonic evolution of south America. Rio de Janeiro, 31st International Geological Congress, 41-95. Available on line at: https://rigeo.cprm.gov.br/handle/doc/19419 / (accessed on 10 November 2022)

Tassinari C.C.G., Macambira M.J.B. 1999. Geochronological provinces of the Amazonian Craton. Episodes, 22, 174-182. https://doi.org/10.18814/epiiugs/1999/v22i3/004

Tassinari C.G.C., Cordani U.G., Nutman A.P., Schmus W.R.V., Bettencourt J.S., Taylor P.N. 1996. Geochronological systematics on basement rocks from the Rio Negro-Juruena Province (Amazonian Craton) and tectonic implications. International Geology Review, 38, 161-175. https://doi.org/10.1080/00206819709465329

Teixeira W., Tassinari C.C.G., Cordani U.G., Kawshita K. 1989. A review of the geochronology of the Amazonian Craton: tectonic implications. Precambrian Research, 42, 213-227. https://doi.org/10.1016/0301-9268(89)90012-0

Toczeck A., Schmitt R.S., Braga M.A.S., Miranda F.P. 2019. Tectonic evolution of the Paleozoic Alto Tapajós intracratonic basin - A case study of a fossil rift in the Amazon Craton. Journal of South American Earth Sciences, 94, 102225. https://doi.org/10.1016/j.jsames.2019.102225

Trevisan V.G., Hagemann S.G., Loucks R.R., Xavier R.P., Motta J.G., Parra-Avila L.A., Petersson A., Gao J.F., Kemp A.I.S., Assis R.R. 2021. Tectonic switches recorded in a Paleoproterozoic accretionary orogen in the Alta Floresta Mineral Province, southern Amazonian Craton. Precambrian Research, 364, 106324. https://doi.org/10.1016/j.precamres.2021.106324

Trindade Netto, G.B., Diener, F.S., Fuentes, D.B.V., REZENDE, E. S. (org). 2020. Áreas de relevante interesse mineral (ARIM): evolução crustal e metalogenia da Região de Aripuanã, estado do Mato Grosso. Goiânia: CPRM. Informe de Recursos Minerais. Série Províncias Minerais do Brasil, 28. Available on line at: https://rigeo.cprm.gov.br/handle/doc/21663 / (accessed on 10 November 2022)

Tucker R.D., Gower C.F. 1994. A U-Pb geochronological framework for the Pinware Terrane, Grenville Province, southeast Labrador. Journal of Geology, 102 (1), 67-78. https://doi.org/10.1086/629648

Vasquez M.L., Sousa C.S., Carvalho, J.M.A. (org.). 2008. Mapa geológico e de recursos minerais do estado do Pará. Belém, CPRM. 1 mapa. Escala 1:1.000.000. Available on line at: http://rigeo.cprm.gov.br/jspui/handle/doc/10443/ (accessed on 17 November 2022)

Wahlgren C.-H., Stephens M.B. 2020. Småland lithotectonic unit dominated by Paleoproterozic (1.8 Ga) syn-orogenic magmatism, Svecokarelian orogen. In: Stephens M.B., Weihed B.J. (eds.). Sweden: lithotectonic framework, tectonic evolution and mineral resources. Geological Society Memoir 50, Geological Society of London, p. 207-235. https://doi.org/10.1144/M50-2017-19

Whitmeyer S.J., Karlstrom K.E. 2007. Tectonic model for the Proterozoic growth of North America. Geosphere, 3 (4), 220-259. https://doi.org/10.1130/GES00055.1

Zhao G., Sun M., Wilde, S.A., Sanzhong L. 2004. A Paleo-Mesoproterozoic supercontinent: assembly, growth and breakup. Earth-Science Reviews, 67, 91–123. https://doi.org/10.1016/j.earscirev.2004.02.003